arXiv:1906.02884v2 [econ.EM] 30 Sep 2019

A long short-term memory stochastic volatility model

Nghia Nguyen* Minh-Ngoc Tran* David Gunawan† Robert Kohn†

December 15, 2024

Abstract

Stochastic Volatility (SV) models are widely used in the financial sector while Long Short-Term Memory (LSTM) models are successfully used in many large-scale industrial applications of Deep Learning. Our article combines these two methods in a non-trivial way and proposes a model, which we call the LSTM-SV model, to capture the dynamics of stochastic volatility. The proposed model overcomes the short-term memory problem in conventional SV models, is able to capture non-linear dependence in the latent volatility process, and often has a better out-of-sample forecast performance than SV models. These properties are illustrated through simulation study and applications to three financial time series datasets: The US stock market weekly index SP500, the Australian stock weekly index ASX200 and the Australian-US dollar daily exchange rates. Based on our analysis, we argue that there are significant differences in the underlying dynamics between the volatility process of the SP500 and ASX200 datasets and that of the exchange rate dataset. For the stock index data, there is strong evidence of long-term memory and non-linear dependence in the volatility process, while this is not the case for the exchange rates. An user-friendly software package together with the examples reported in the paper are available at `https://github.com/vbayeslab`.

1 Introduction

The volatility of a financial time series, such as stock returns or exchange rates, at a particular time point or during a particular time interval, is defined as the variance of the returns and serves as a measure of the uncertainty about the returns. The volatility, which is often of great interest to financial econometricians, is unobserved so that it is necessary to model it statistically in order to estimate it. The two model classes most frequently used in volatility modelling are the Generalized Autoregressive Conditional Heteroscedastic (GARCH) models and the Stochastic Volatility (SV) models. The GARCH model (Bollerslev, 1986) expresses the current volatility, conditional on the previous returns and volatilities, as a *deterministic* and linear function of the squared return and the conditional volatility in the previous time period. The SV model (Taylor, 1982, 1986), on the other hand, use a latent stochastic process to model the volatility, which is usually taken as a first order autoregressive process. It is well documented that the GARCH and SV models are able to capture important effects

*Discipline of Business Analytics, The University of Sydney Business School and ACEMS.
†School of Economics, UNSW Business School and ACEMS.

exhibited in the variance of financial returns. For example, the volatilities in financial returns are observed to be highly autocorrelated in certain time periods and exhibit periods of both low and high volatility (Mandelbrot, 1967). This so-called volatility clustering phenomenon can be modeled by the volatility processes introduced in the GARCH and SV models, making these volatility models widely employed in financial time series modelling.

Although the GARCH and SV models were independently and almost concurrently introduced, the GARCH models were initially more widely adopted as it is much easier to estimate GARCH models than SV models. This is because the likelihood of a GARCH model can be obtained explicitly, while the likelihood of a SV model is intractable as it is an integral over the latent volatilities. However, the conditional variance process of GARCH models is deterministic and hence GARCH models might not capture efficiently the random oscillatory behavior of financial volatility (Nelson, 1991). SV models are considered as an attractive alternative to GARCH models because they overcome this limitation (Kim et al., 1998; Yu, 2002). Recent advances in Bayesian computation such as particle Markov chain Monte Carlo (PMCMC) (Andrieu et al., 2010) allow straightforward estimation and inference for such models.

Standard SV models (Taylor, 1982) still cannot appropriately capture some important features naturally arising in financial volatility. For example, a large amount of both theoretical and empirical evidence indicates that there exists long-range persistence in the volatility process of many financial returns, see, e.g, Lo (1991), Ding et al. (1993), Crato and de Lima (1994), Bollerslev and Mikkelsen (1996). The long-memory property of a time series implies that the decay of the autocorrelations of the series is slower than exponential. The standard SV model uses an AR(1) process to model the log of the volatility and hence might fail to capture this type of persistence (Breidt et al., 1998). Another line of the literature shows strong evidence of non-linear auto-dependence in the volatility process of some stock and currency exchange returns (Kiliç, 2011) and that the simple linear AR(1) process cannot effectively capture the underlying non-linear volatility dynamics.

Breidt et al. (1998) proposed the Long Memory Stochastic Volatility (LMSV) model to overcome the short-memory limitation of the standard SV model. LMSV incorporates an ARFIMA process (Granger and Joyeux, 1980) as an alternative to the AR(1) process to capture the long-memory dependence of the conditional volatility. The empirical evidence in Breidt et al. (1998) suggests that the LMSV model is able to reproduce the long-memory volatility behavior in some stock return datasets. However, the literature is unclear on whether the LMSV model can capture non-linear dynamics within the volatility process, because the ARFIMA model is linear. Additionally, it is challenging to estimate the LMSV model as its likelihood is intractable. We are unaware of any available software package that implements the LMSV methodology. In another approach, Yu et al. (2006) introduced a family of non-linear SV (N-SV) models to capture the possible departure from the log transform commonly used in SV models. In the standard SV model, the logarithm of volatility is assumed to follow an AR(1) process; N-SV uses other non-linear transformations, such as the Box-Cox power function, of the volatility. The simulation studies and empirical results on currency exchange and option pricing data in Yu et al. (2006) show that the N-SV model using the Box-Cox transformation is able to detect some interesting effects in the underlying volatility process. The general use of N-SV models requires the user to select an appropriate non-linear transformation for the dataset under consideration, and this might lead to a challenging model selection problem. Both Breidt et al. (1998) and Yu et al. (2006) did not clearly discuss the

out-of-sample forecast performance of their LMSV and N-SV models.

Recurrent neural networks (RNN) including the Long Short-Term Memory (LSTM) model of Hochreiter and Schmidhuber (1997) in the Deep Learning literature have been successfully deployed in a large number of industrial-level applications (language translation, image captioning, speech synthesis, etc.). The LSTM model and its variants are well-known for their ability to efficiently capture the long-range memory and non-linear dependence existing within various types of sequential data, and are considered as the state-of-the-art models for many sequence learning problems (Lipton et al., 2015). Many researchers and practitioners have used Deep Learning techniques for price forecasting in financial time series analysis, but the general consensus is that these machine learning models do not clearly outperform the traditional time series models such as ARMA and ARIMA (see, e.g., Makridakis et al. (2018); Zhang (2003)). Makridakis et al. (2018) note that without careful modifications, Machine Learning models are usually less accurate than the statistical approaches that have been extensively investigated in the financial time series literature. We are unaware of any existing work that uses RNN to model the latent volatility dynamics. There are two reasons for this lack of research. First, it is non-trivial to sensibly incorporate RNN into statistical volatility models. Simple adaptations of RNN to volatility models easily overlook the important stylized facts exhibited in financial volatility such as volatility clustering. Second, a volatility model that incorporates a RNN into its latent process is highly sophisticated and thus challenging to estimate.

This paper combines the SV and LSTM models in a non-trivial way, and proposes a new model, called the LSTM-SV model. The LSTM-SV model retains the essential components of the SV model and improves it by using the LSTM model to capture the potential long-memory and non-linear dependence in the volatility dynamics that cannot be picked up by an AR(1) process. The LSTM-SV model belongs to the class of state space models whose Bayesian inference can be performed using recent advances in the particle MCMC literature (Andrieu and Roberts, 2009; Andrieu et al., 2010). The simulation studies and empirical results on stock returns and currency exchange rates suggest that the LSTM-SV model can efficiently capture the potential non-linear and long-memory effects in the underlying volatility dynamics, and provide better out-of-sample forecasts than the standard SV and N-SV models. A Matlab software package implementing Bayesian estimation and inference for LSTM-SV together with the examples reported in this paper are available at `https://github.com/vbayeslab`.

The article is organized as follows. Section 2 briefly reviews the SV and LSTM models, and presents the LSTM-SV model. Section 3 discusses in detail Bayesian estimation and inference for the LSTM-SV model. Section 4 presents the simulation study and applies the LSTM-SV model to analyze three benchmark financial datasets. Section 5 concludes. The Appendix gives details of the implementation and further empirical results.

2 The LSTM-SV model

2.1 The SV model and its possible weaknesses

Let $y = \{y_t,\ t = 1, ..., T\}$ be a series of financial returns. We consider a basic version of SV models (Taylor, 1982)

$$y_t = e^{\frac{1}{2}z_t}\epsilon_t^y,\ \ \epsilon_t^y \sim \mathcal{N}(0,1),\ \ t = 1, 2, ..., T \tag{1}$$

$$z_t = \mu + \phi(z_{t-1} - \mu) + \epsilon_t^z,\ \ \epsilon_t^z \sim \mathcal{N}(0, \sigma^2),\ \ t = 2, ..., T,\quad z_1 \sim \mathcal{N}\Big(\mu, \frac{\sigma^2}{1-\phi^2}\Big). \tag{2}$$

The persistence parameter ϕ is assumed to be in $(-1,1)$ to enforce stationarity of both the z and y processes. In this SV model, the volatility process z is assumed to follow an AR(1) model. It is well documented in the financial econometrics literature that financial time series data often exhibit a long-term dependence, which forces the persistence parameter ϕ to be close to 1 (Jacquier et al., 1994; Kim et al., 1998). Write $p(z|\theta)$ for the density of z given the model parameters $\theta = (\mu, \phi, \sigma^2)$ and $p(y|z)$ for the density of the data y conditional on z. We can view $p(z|\theta)$ as the prior with θ being the hyper-parameters and $p(y|z)$ as the likelihood (Jacquier et al., 1994). Under this perspective, the SV model (1)-(2) puts non-zero prior mass on AR(1) stochastic processes, and zero or almost-zero mass on stochastic processes that are far from being well approximated by an AR(1). This means that the SV model in (1)-(2) might be not able to capture more complex dynamics, such as long-term memory or non-linear auto-dependence, in the posterior behavior of the volatility process z, and that a more flexible prior distribution should be put on z. We will design such a flexible prior by combining the attractive features from both SV and LSTM time series modeling techniques.

Yu et al. (2006) proposed the class of non-linearity N-SV models as a variant of SV which allows a more flexible link between the variance $\text{Var}(y_t|z_t)$ and the AR(1) process z. Their N-SV model, using the Box-Cox transformation for $\text{Var}(y_t|z_t)$, is written as

$$y_t = (1 + \delta z_t)^{1/2\delta}\epsilon_t^y,\ \ \epsilon_t^y \sim \mathcal{N}(0,1),\ \ t = 1, 2, ..., T \tag{3}$$

$$z_t = \mu + \phi(z_{t-1} - \mu) + \epsilon_t^z,\ \ \epsilon_t^z \sim \mathcal{N}(0, \sigma^2),\ \ t = 2, ..., T,\quad z_1 \sim \mathcal{N}\Big(\mu, \frac{\sigma^2}{1-\phi^2}\Big), \tag{4}$$

where δ is the auxiliary parameter that measures the degree of non-linearity rather than the log transform. As $\delta \to 0$, $(1+\delta z_t)^{1/2\delta} \to e^{\frac{1}{2}z_t}$ and hence the N-SV model includes the SV model as a special case. The term non-linearity here might cause some confusion, as it does not refer to the non-linear auto-dependence within the volatility process z, but any non-linearity transforms, including the log transform, in the standard SV model. Our article will use the standard SV and N-SV models as the benchmarks to evaluate the LSTM-SV model.

2.2 The LSTM model

There are at least two approaches to modeling time series data. One approach is to represent time effects *explicitly* via some simple function, often a linear function, of the lagged values of the time series. This is the mainstream time series data analysis approach in the statistics literature with the well-known models such as AR or ARMA. The alternative approach is to represent time effects *implicitly* via latent variables, which are designed to store the memory

of the dynamics in the data. These latent variables, also called hidden states, are updated in a recurrent manner using the information carried over by their values from the previous time steps and the information from the data at the current time step. Recurrent neural networks (RNN), belong to the second category, were first developed in cognitive science and successfully used in computer science. Another class of models that represent time implicitly is state space models, which are widely used in econometrics and statistics. The SV model discussed in Section 2.1 is an example of state space models.

For the purpose of this section, denote our time series data as $\{D_t = (x_t, z_t),\ t = 1,2,...\}$ where x_t is the vector of inputs and z_t the output. In our article, it is useful to think of x_t as scalar; however, the LSTM approach is often efficiently used to model multivariate time series. If the time series of interest has the form $\{z_t,\ t=1,2,...\}$, it can be written as $\{(x_t, z_t),\ t=2,...\}$ with $x_t = z_{t-1}$. Our goal is to model the conditional distribution $p(z_t|x_t, D_{1:t-1})$. If the serial dependence structure is ignored, then a feedforward neural network (FNN) can be used to transform the raw input data x_t into a set of hidden units h_t, often called *learned features*, for the purpose of explaining or predicting z_t. However, this approach is unsuitable for time series data as the time effects or the serial correlations are totally ignored. The main idea behind RNN is to let the set of hidden units h_t to feed itself using its lagged value h_{t-1} from the previous time step $t-1$. Hence, RNN can be best thought of as a FNN that allows a connection of the hidden units to their value from the previous time step, enabling the network to possess memory. Mathematically, this RNN model (Elman, 1990) is written as

$$\begin{aligned} h_t &= \mathcal{H}(vx_t + wh_{t-1} + b), && (5)\\ \eta_t &= \beta_0 + \beta_1 h_t, && (6)\\ z_t|\eta_t &\sim p(z_t|\eta_t). && (7) \end{aligned}$$

In (5)-(7), v, w, b, β_0 and β_1 are model parameters, $\mathcal{H}(\cdot)$ is a non-linear activation function, e.g., common choices for $\mathcal{H}(\cdot)$ are the sigmoid $\sigma(z) = 1/(1+e^{-z})$ and the *tanh* $\phi(z) = (e^z - e^{-z})/(e^z + e^{-z})$ functions, and $p(z_t|\eta_t)$ is a distribution depending on the learning task. For example, if z_t is continuous, then typically $p(z_t|\eta_t)$ is a normal distribution with mean η_t; if z_t is binary, then $z_t|\eta_t$ follows a Bernoulli distribution with probability $\sigma(\eta_t)$.Usually we can set $h_1 = 0$, i.e. the neural network initially does not have any memory.

Figure 1 illustrates graphically the RNN model (5)-(7). We follow Goodfellow et al. (2016) and use a black square to indicate the delay of a single time step in the circuit diagram (*Left*). The circuit diagram can be interpreted as an unfolded computational graph (*Right*), where each node is associated with a particular time step. The unfolded graph in Figure 1 suggests that the hidden state at time t is the output of a composite function

$$h_t = f\Big(x_t, f(x_{t-1}, ..., f(x_1, h_0))\Big), \text{ where } f(x_t, h_{t-1}) := \mathcal{H}(vx_t + wh_{t-1} + b). \quad (8)$$

Denote $L_t(z_t)$ the loss function (e.g. square loss if z_t is continuous) of the model (5)-(7) at time step t, one can calculate the gradient of L_t with respect to a model parameter W, using the the chain rule, as

$$\begin{aligned} \frac{\partial L_t}{\partial W} &= \frac{\partial L_t}{\partial z_t}\frac{\partial z_t}{\partial \eta_t}\frac{\partial \eta_t}{\partial h_t}\frac{\partial h_t}{\partial h_{t-1}}\cdots\frac{\partial h_2}{\partial h_1}\frac{\partial h_1}{\partial W} && (9)\\ &= \frac{\partial L_t}{\partial z_t}\frac{\partial z_t}{\partial \eta_t}\frac{\partial \eta_t}{\partial h_t}\left[\prod_{i=2}^{t}\mathcal{H}'(vx_i + wh_{i-1} + b)\right]w^{t-1}\frac{\partial h_1}{\partial W}, && (10) \end{aligned}$$

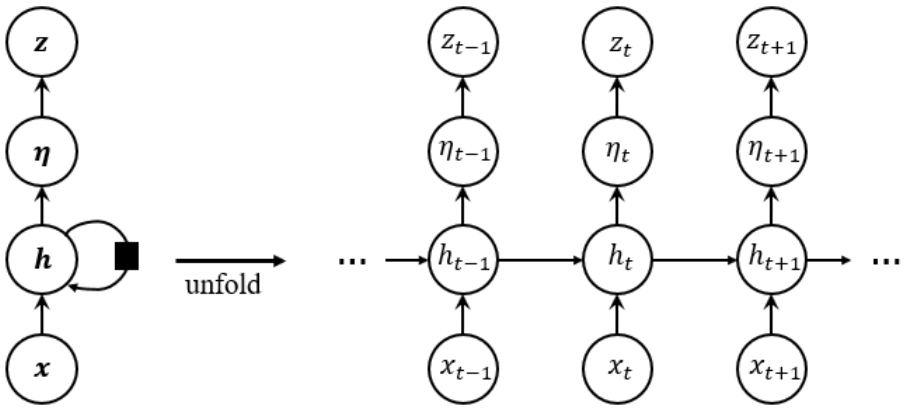

Figure 1: Graphical representation of the RNN model in (5)-(7).

where $\mathcal{H}'(\cdot)$ is the derivative of the activation function $\mathcal{H}(\cdot)$. We note that the derivative $\mathcal{H}'(\cdot)$ is always between 0 and 1 if $\mathcal{H}(\cdot)$ is the tanh or sigmoid activation function. Consequently, the gradient in (10) might either explode or vanish if t is sufficiently large and w is not equal to 1, as the exponentially fast decay or growth factor w^{t-1} is the most dominant term in (10) (Bengio et al., 1993, 1994). The exploding gradient problem occurs when the gradient gets too large, thus making the optimization for the model parameters (e.g., using gradient descent) highly unstable. The vanishing gradient problem occurs when the gradient is close to zero, making the learning process too slow as the earlier hidden states have little effect on the later ones. The difficulty caused by an exploding and vanishing gradient explains why the basic RNN is inefficient in learning long-term dependence in long data sequences (Hochreiter and Schmidhuber, 1997). The exploding gradient problem does not commonly arise in practice and can be easily overcome, for example, by setting a threshold on the gradient to prevent it from getting too large (Bengio et al., 1994). A vanishing gradient, however, is a much more serious problem.

The LSTM model was proposed in Hochreiter and Schmidhuber (1997) (see also Gers et al. (2000)) as the most efficient solution to mitigate the vanishing gradient problem. The LSTM model extends the basic RNN by introducing three extra hidden units, called the input gate, output gate and forget gate, that work with each other to control the flow of information through the network. The left diagram in Figure 2 illustrates the structure of a Simple Recurrent Network (SRN) such as that in Equation (5)-(7), and the right diagram shows the structure of a LSTM cell. Mathematically, this LSTM cell is written as

$$
\begin{aligned}
g_t^f &= \sigma(v_f x_t + w_f h_{t-1} + b_f) && \text{Forget Gate} && (11)\\
g_t^i &= \sigma(v_i x_t + w_i h_{t-1} + b_i) && \text{Input Gate} && (12)\\
x_t^d &= \sigma(v_d x_t + w_d h_{t-1} + b_d) && \text{Data Input} && (13)\\
g_t^o &= \sigma(v_o x_t + w_o h_{t-1} + b_o) && \text{Output Gate} && (14)\\
C_t &= g_t^f \odot C_{t-1} + g_t^i \odot x_t^d && \text{Cell State} && (15)\\
h_t &= g_t^o \odot tanh(C_t) && \text{Cell Output} && (16)
\end{aligned}
$$

where $\sigma(\cdot)$ is the sigmoid function and $\odot$ denotes element-wise multiplicative operation. The cell state C_t, which also operates in a recurrent manner, is the most crucial part that helps

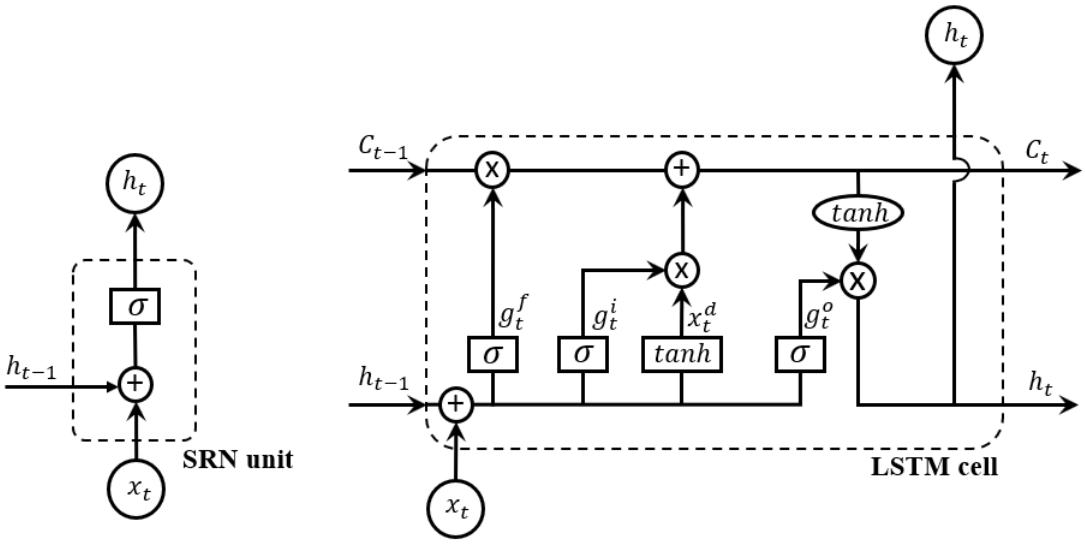

Figure 2: The structure of the SRN unit (*left*) and LSTM cell (*right*). The $\oplus$ and $\otimes$ symbols represent the addition and multiplication operation, respectively.

LSTM to mitigate the vanishing gradient problem. Similarly to (9)-(10), it is straightforward to derive the gradient $\partial L_t/\partial W$ of the LSTM model in (11)-(16) as

$$\frac{\partial L_t}{\partial W} = \frac{\partial L_t}{\partial z_t}\frac{\partial z_t}{\partial \eta_t}\frac{\partial \eta_t}{\partial h_t}\frac{\partial h_t}{\partial C_t}\frac{\partial C_t}{\partial C_{t-1}}\cdots\frac{\partial C_2}{\partial C_1}\frac{\partial C_1}{\partial W} \tag{17}$$

$$= \frac{\partial L_t}{\partial z_t}\frac{\partial z_t}{\partial \eta_t}\frac{\partial \eta_t}{\partial h_t}\left[\prod_{i=2}^{t}(g_i^f + \widetilde{C}_{i-1})\right]\frac{\partial h_1}{\partial W}, \tag{18}$$

where $\widetilde{C}_{i-1}$ represents the remaining terms of $\partial C_i/\partial C_{i-1}$ as g_t^f,g_t^i,x_t^d are also functions of h_{t-1}, and hence C_{t-1}. Clearly the gradient in (18) does not involve any exponentially fast decay or growth factors as the gradient in the simple RNN (10) shows, and hence effectively protects the network from the gradient vanishing and exploding problem. More specifically, the special structure of LSTM allows the gates g_t^f, g_t^i and g_t^o to adaptively change their values to keep the product term in (18) from converging to zero as t increases. In this manner, the network learns to decide when to forget unimportant information (by letting the corresponding gradients to vanish) and when to keep important information (by preserving the corresponding gradients) during the training process on long data sequences. Hence, the RNN network with LSTM cells can efficiently capture non-linear and long-range dependence often exhibited in sequential data such as text, voice or video. See Hochreiter and Schmidhuber (1997), Gers et al. (2000) , and Goodfellow et al. (2016) for a more comprehensive discussion on how LSTM networks work and overcome the limitations in the basic RNN networks.

We denote the functional learning structure in (11)-(16) as h_t=LSTM(x_t,h_{t-1}), which takes x_t, the data at time t, and h_{t-1}, the output of LSTM cell at time $t-1$, as input arguments. For a discussion on variants of LSTM see, for example, Goodfellow et al. (2016) and Greff et al. (2017).

2.3 The LSTM-SV model

This section proposes the LSTM-SV model that combines SV and LSTM for financial volatility modelling. The key idea is that we use LSTM to model the long-term memory and non-linear auto-dependence in the volatility dynamics that cannot be picked up by the basic SV model. This leads to a prior distribution for the volatility process z that is much more flexible than the AR(1) prior (c.f. Section 2.1). The LSTM-SV model is written as

$$
\begin{aligned}
y_t &= e^{\frac{1}{2}z_t}\epsilon_t^y, \;\; \epsilon_t^y \overset{iid}{\sim} \mathcal{N}(0,1), \;\; t=1,2,...,T && (19)\\
z_t &= \eta_t + \phi z_{t-1}, \;\; t=2,...,T, \;\; z_1 = \eta_1 + \phi z_0 && (20)\\
\eta_t &= \beta_0 + \beta_1 h_t + \epsilon_t^\eta, \;\; \epsilon_t^\eta \overset{iid}{\sim} \mathcal{N}(0,\sigma^2), \;\; t=1,2,...,T && (21)\\
h_t &= \text{LSTM}(\eta_{t-1}, h_{t-1}), \;\; t=2,...,T, \;\; \text{with } h_1 := 0, && (22)
\end{aligned}
$$

where z_0 is the initial value of the log volatility process and a convenience choice of z_0 is the log of the unconditional variance of the given sample series y, i.e., $z_0 = \log(\text{var}(y))$. We follow the LSTM literature to initialize $h_1 = 0$ as the LSTM cell initially has no memory. This model retains the measurement equation (19) and the linear part in the AR(1) process from the standard SV model, and captures the non-linear and long-memory part $\eta_t = z_t - \phi z_{t-1}$ by the LSTM structure. We therefore follow the SV literature and assume that $|\phi| < 1$. If $\beta_1 = 0$ and $\epsilon_1^\eta \sim \mathcal{N}(\beta_0/(1-\phi), \sigma^2/(1-\phi^2))$, the LSTM-SV model (19)-(22) becomes the SV model (1)-(2) and hence the SV model is a special case of the LSTM-SV model. The z process and thus the y process of the LSTM-SV model, is not guaranteed to be stationary unless $\beta_1 = 0$ and $\epsilon_1^\eta \sim \mathcal{N}(\beta_0/(1-\phi), \sigma^2/(1-\phi^2))$. Non-stationarity for volatility is often argued to be more realistic in practice (e.g. van Bellegem (2012)), although it maybe mathematically less appealing as then concepts such as autocorrelation and constant variance no longer apply. We note that the process z_t in the LSTM-SV model does not explode because h_t is always between -1 and 1. The vector of model parameters θ consists of β_0, β_1, ϕ, σ^2 and the parameters in the LSTM model. The Appendix contains the graphical representation and fully written out version of the LSTM-SV model in (19)-(22). The parameter β_1 measures all the effects in the underlying volatility process z rather than the linear effect captured by the AR(1) process. We refer to β_1 as the non-linearity long-memory coefficient. It might be interesting to develop a test of the null hypothesis that $\beta_1 = 0$, which is equivalently a goodness of fit test to the data between the SV and LSTM-SV models. However, we do not pursue this idea further in this paper. Finally, β_0 plays the role of the scale factor $\tau = e^{\beta_0/2}$ for the variance of y_t. One could set $\beta_0 = 0$ and modify (19) to $y_t = \tau e^{\frac{1}{2}z_t}\epsilon_t^y$; however, this parameterization might be less statistically efficient in terms of Bayesian estimation, especially for the parameter τ (see Kim et al., 1998).

It is straightforward to extend the LSTM-SV model in (19)-(22) by incorporating other advances in the SV literature. For example, we can use a Student-t distribution instead of a Gaussian for the measurement shock ϵ_t^y and take into account the leverage effect by correlating ϵ_t^y with the volatility shock ϵ_t^η. We do not consider these extensions here, because using the most basic version makes it easier to understand the strengths and weaknesses of the new model.

3 Bayesian inference

This section discusses Bayesian estimation and inference for the LSTM-SV model. For a generic sequence $\{x_t\}$ we use $x_{i:j}$ to denote the series $(x_i,...,x_j)$. The LSTM-SV model is a state-space model with the measurement equation

$$y_t|z_t \sim \mathcal{N}(0, e^{z_t}) \tag{23}$$

and the state transition equation

$$z_t|z_{1:t-1}, h_t \sim \mathcal{N}(\phi z_{t-1} + \beta_0 + \beta_1 h_t, \sigma^2), \quad t \geq 2, \quad z_1 \sim \mathcal{N}(\beta_0, \sigma^2). \tag{24}$$

We are interested in sampling from the posterior distribution of θ

$$p(\theta|y_{1:T}) = \frac{p(y_{1:T}|\theta)p(\theta)}{p(y_{1:T})}, \tag{25}$$

where $p(y_{1:T}|\theta)$ is the likelihood function, $p(\theta)$ is the prior and $p(y_{1:T}) = \int_\Theta p(y_{1:T}|\theta)p(\theta)d\theta$ is the marginal likelihood. Recall that the vector of model parameters θ consists of β_0, β_1, ϕ, σ^2 and the 12 parameters within the LSTM model (11)-(16).

The likelihood function in (25) is

$$p(y_{1:T}|\theta) = \int p(y_{1:T}|z_{1:T}, \theta)p(z_{1:T}|\theta)dz_{1:T} \tag{26}$$

which is computationally intractable for non-linear, non-Gaussian state space models like the SV and LSTM-SV models. Andrieu et al. (2010) proposed the pseudo-marginal MCMC method for Bayesian inference in state space models, in which the intractable likelihood is estimated unbiasedly by a particle filter. Denote by $\widehat{p}(y_{1:T}|\theta,u)$ the unbiased estimator of the likelihood $p(y_{1:T}|\theta)$, with u the set of pseudo random numbers used within the particle filter to estimate the likelihood. The pseudo-marginal MCMC sampler accepts a proposal (θ',u') with the acceptance probability

$$1 \wedge \frac{\widehat{p}(y_{1:T}|\theta', u')}{\widehat{p}(y_{1:T}|\theta, u)} \frac{p(\theta')}{p(\theta)} \frac{q(\theta|\theta')}{q(\theta'|\theta)}. \tag{27}$$

The efficiency of particle MCMC depends on the variance of the estimated likelihood, and hence on the number of particles used in the particle filter. Pitt et al. (2012) suggests that the pseudo-marginal MCMC approach works efficiently when the variance of the log of the estimated likelihood is around 1. For some state space models like the LSTM-SV model, a large number of particles might be required to obtain a likelihood estimator with log variance to be around 1. To tackle this problem, Tran et al. (2016) proposed the Block Pseudo-Marginal (BPM) approach that updates the pseudo-random numbers u in blocks. That is, BPM divides u into blocks and updates θ together with one block of u at a time in a component-wise MCMC manner. This blocking strategy makes the current u and proposal u' correlated, and helps reduce the variance of the ratio $\widehat{p}(y_{1:T}|\theta',u')/\widehat{p}(y_{1:T}|\theta,u)$ in (27), thus leading to a better mixing Markov chain. See Deligiannidis et al. (2018) for an alternative way of correlating u and u'.

Section 3.1 discusses in detail the BPM sampler for sampling in LSTM-SV and Section 3.2 shows how to compute the marginal likelihood of the LSTM-SV model using the Importance Sampling Squared method of Tran et al. (2019).

3.1 The Block Pseudo-Marginal Algorithm

Let u be the vector of random numbers used in the particle filter for computing the likelihood estimate $\widehat{p}(y_{1:T}|\theta,u)$. BPM divides u into G blocks $u=(u_{(1)},...,u_{(G)})$. Algorithm 1 summarizes the BPM sampler for sampling from the posterior distribution of the model parameters θ in the LSTM-SV model.

Algorithm 1 Block Pseudo-Marginal Algorithm

For each MCMC iteration:

1. Sample θ' from the proposal density $q(\theta'|\theta)$.
2. Sample the block index K with $\Pr(K=k)=1/G$ for any $k=1,...,G$.
   Sample $u'_{(K)} \sim \mathcal{N}(0,I_{d_K})$ where I_{d_K} is the identity matrix of size d_K with d_K the length of block $u_{(K)}$. Set $u'=(u_{(1)},...,u_{(K-1)},u'_{(K)},u_{(K+1)},...,u_{(G)})$.
3. Compute the estimated likelihood $\widehat{p}(y_{1:T}|\theta',u')$ using a particle filter (see Algorithm 3 in the Appendix).
4. Accept the proposal (θ',u') with the probability

$$\min\left\{1, \frac{\widehat{p}(y_{1:T}|\theta',u')}{\widehat{p}(y_{1:T}|\theta,u)} \frac{p(\theta')}{p(\theta)} \frac{q(\theta|\theta')}{q(\theta'|\theta)}\right\}.$$

Tran et al. (2016) showed that the correlation between the logs of the estimated likelihood at the proposed and current values of model parameters is approximately $\rho=1-\frac{1}{G}$. If G is set too large, then some blocks $u_{(k)}$ might be not updated, making the Markov chain unduly depend on the initial u and the resulting posterior samples may not be from the correct target posterior. If G is too small, then the correlation ρ will be too small and it will generally be difficult to accept proposed values of θ. In this paper, we set $G=200$ as the default value which is large enough to produce stable results for the LSTM-SV model. However, users may set different values for G in our software package.

We use a random walk proposal for $q(\theta'|\theta)$ and follow Garthwaite et al. (2010) to adaptively modify the covariance matrix in the random walk proposal by a scaling factor. This enables us to robustly maintain a specified overall acceptance probability. In the examples, we set this overall acceptance probability to be 25%

3.2 Model choice by marginal likelihood

The marginal likelihood is often used to choose between models (Good, 1952). We estimate the marginal likelihood of the LSTM-SV model using the importance sampling squared (IS^2) method of Tran et al. (2019). Using the samples of θ from the BPM sampler, we construct a proposal density $g_{IS}(\theta)$ for θ, which we choose to be a mixture of normal densities and use Algorithm 2 to estimate the marginal likelihood $p(y_{1:T})$. Step 1 in Algorithm 2 is parallelizable, which makes the IS^2 method computationally efficient for estimating the marginal likelihood, especially when we can construct a good proposal density based on samples from BPM. Tran

et al. (2019) show that the IS^2 estimator of the marginal likelihood is unbiased, has a finite variance and is asymptotically normal.

Algorithm 2 IS^2 algorithm

1. For $i=1,...,M$

   (a) Sample $\theta_i \overset{iid}{\sim} g_{IS}(\theta)$.

   (b) Calculate the estimated likelihood $\widehat{p}(y_{1:T}|\theta_i)$ of θ_i using a particle filter (see Algorithm 3 in the Appendix).

   (c) Compute the importance weight for each θ_i

$$\widetilde{w}(\theta_i) = \frac{p(\theta_i)\widehat{p}(y_{1:T}|\theta_i)}{g_{IS}(\theta_i)}.$$

2. The marginal likelihood estimated is

$$\widehat{p}_{IS^2}(y_{1:T}) = \frac{1}{M}\sum_{i=1}^{M}\widetilde{w}(\theta_i).$$

4 Simulation studies and applications

This section evaluates the performance of the LSTM-SV model relative to the SV and N-SV models using a simulation study and real data applications. The BMP sampler is used to perform Bayesian inference and the IS^2 algorithm is used to estimate the marginal likelihood in all models. Table 1 lists the priors for the LSTM-SV, SV and N-SV model parameters for all the examples. For the BPM sampler, we use $N=200$ particles in the particle filter (Algorithm 3) to compute the estimated likelihood and divide the set of random numbers u into $G=200$ blocks. Each block is a vector that is roughly of length $N \times \frac{T}{G}$, where T is the length of the time series. In all the examples, we ran the BPM sampler using 100,000 MCMC iterations, then discarded the first 10,000 iterations as burn-ins and thinned the rest by keeping every 5th iteration. The BPM sampler was initialized by sampling from the priors in Table 1.

We now motivate the choice of the priors in Table 1. We follow Yu et al. (2006) and Kim et al. (1998) to set the same prior, which is a Beta distribution, for the persistence parameters ϕ of the three models. We also use an inverse-Gamma prior for the parameters σ^2 in the three models but make it more flat than the priors used in Yu et al. (2006) and Kim et al. (1998). We follow Yu et al. (2006) to use an informative but reasonably flat prior distribution for the intercept μ in the SV and N-SV models. For the LSTM-SV model, we found that the posterior distribution of β_1 to be unimodal under an inverse-Gamma prior. We also observed that the BPM sampler runs more stably under an inverse-Gamma prior than other choices, e.g., a Gamma distribution, of the prior of β_1. We use a normal prior with a zero mean and a small variance for the LSTM parameters because empirical results from the LSTM literature show that the values of the LSTM parameters are often small. Finally, we set a normal prior

LSTM-SV		SV		N-SV	
Parameter	Prior	Parameter	Prior	Parameter	Prior
β_0	$\mathcal{N}(0,0.01)$	μ	$\mathcal{N}(0,25)$	μ	$\mathcal{N}(0,25)$
$\frac{\phi+1}{2}$	Beta(20,1.5)	$\frac{\phi+1}{2}$	Beta(20,1.5)	$\frac{\phi+1}{2}$	Beta(20,1.5)
σ^2	$IG(2.5,0.25)$	σ^2	$IG(2.5,0.25)$	σ^2	$IG(2.5,0.25)$
β_1	$IG(2.5,0.25)$			δ	$\mathcal{N}(0,0.1)$
v_f,v_i,v_d,v_o	$\mathcal{N}(0,0.1)$				
w_f,w_i,w_d,w_o	$\mathcal{N}(0,0.1)$				
b_f,b_i,b_d,b_o	$\mathcal{N}(0,0.1)$				

Table 1: Prior distributions for the parameters in the LSTM-SV, SV and N-SV models. The notation $\mathcal{N}$, IG and Beta denote the Gaussian, inverse-Gamma and Beta distributions, respectively.

with a zero mean and a small variance for the intercept β_0 in the LSTM-SV model as the empirical results often show small values of β_0.

We use $N_{\text{IS}^2} = 2000$ particles and $M_{\text{IS}^2} = 5000$ importance samples of θ to estimate the marginal likelihood in the IS^2 algorithm. The number of particles N_{IS^2} and the number of importance samples M_{IS^2} are set to keep the variances of the likelihood estimates in the IS^2 algorithm sufficiently small.

We use the following four predictive scores to measure the out-of-sample performance. The first is the partial predictive score (Gneiting and Raftery, 2007) evaluated on a test dataset D_{test},

$$PPS = -\frac{1}{T_{test}} \sum_{D_{test}} \log p(y_t | y_{1:t-1}, \widehat{\theta}),$$

where T_{test} is the number of observations in D_{test} and $\widehat{\theta}$ is a posterior mean estimate of θ. The model with smallest PPS is preferred. The second predictive score is the number of violations (# violations) defined as the number of times over the test data D_{test} that the observation y_t is outside its 99% one-step-ahead forecast interval.

Our third predictive measure is the quantile score (QS) (Taylor, 2019). One of the main applications of volatility modelling is to forecast the Value at Risk (VaR). The α-VaR is defined as the α-quantile of the one-step-ahead forecast distribution $p(y_t | y_{1:t-1}, \widehat{\theta})$. The performance of a method that produces VaR forecasts is often measured by the quantile score defined as

$$QS = \frac{1}{T_{test}} \sum_{D_{test}} (\alpha - I_{y_t \leq q_{t,\alpha}})(y_t - q_{t,\alpha}),$$

where $q_{t,\alpha}$ is the α-VaR forecast of y_t, conditional on $y_{1:t-1}$. The smaller the quantile score, the better the VaR forecast. We follow Taylor (2019) and use the hit percentage, defined as the percentage of the y_t in the test data that is below its α-VaR forecast, as the fourth predictive score. The hit percentage is expected to be close to α, if the model predicts well.

We note that these predictive performance measures complement each other. For example, it is possible to make the number of violations small by increasing the forecast volatility, but

this increases the PPS and QS scores. A volatility model that minimizes all three predictive scores, and has a hit percentage close to α, is arguably the preferred one.

All the examples were implemented in Matlab and users can easily run the BPM and IS^2 algorithms for the LSTM-SV model on a desktop computer with a moderate hardware configuration using our software package.

4.1 Simulation studies

We consider the following non-linear stochastic volatility model:

$$z_t = 0.1 + 0.96 z_{t-1} - 0.8 \frac{z_{t-1}^2}{1+z_{t-1}^2} + \frac{1}{1+e^{-z_{t-1}}} + \sigma \epsilon_t^z, \quad t = 2, ..., T, \quad z_1 \sim \mathcal{N}(0,1) \tag{28}$$

$$y_t = \exp\left(\frac{1}{2} z_t\right) \epsilon_t^y, \quad t = 1, 2, ..., T, \tag{29}$$

where $\sigma^2 = 0.1$, $\epsilon_t^z \sim \mathcal{N}(0,1)$ and $\epsilon_t^y \sim \mathcal{N}(0,1)$. These parameters are set so that y_t somewhat resembles real financial time series data exhibiting volatility clustering. This data generating process is a modification of the standard SV model by adding two non-linear components to the volatility process.

We generated a time series of 2000 observations from the model in (28) and (29), with the first $T = 1000$ used for model estimation and the second 1000 for out-of-sample analysis. Table 2 shows the posterior mean estimates for the parameters of the SV, N-SV and LSTM-SV models, with the posterior standard deviations in brackets; for the LSTM-SV model we only show the results for the main parameters and put the LSTM parameters in Table 10 in the Appendix. The last column in the table shows the marginal likelihood estimated by the IS^2 algorithm outlined in Section 3.2, averaged over 10 different runs of the IS^2 algorithm, together with the Monte Carlo standard errors in the brackets. The efficiency of the BPM sampler is measured by the Integrated Autocorrelation Time (IACT) (Liu, 2001), which is computed using the CODA R package of Plummer et al. (2006). The IACT is often used to evaluate the computational efficiency of a MCMC sampler. A sampler producing Markov chains with low IACT values is considered to be efficient.

Table 2 shows the IACT values for several of the parameters and suggests the following conclusions. First, the small IACT values across the three models show that BPM is an efficient sampler for these state-space models. In general, the N-SV parameters have higher IACT values since this model does not impose any constraints to ensure the positivity of the conditional volatility and hence makes the estimation process more challenging. Second, all the Monte Carlo standard errors (shown in brackets) of the estimated log marginal likelihood are small, which illustrates the efficiency of IS^2 as a method for marginal likelihood estimation. Third, the LSTM-SV model has the highest marginal likelihood among the three models, suggesting that the LSTM-SV model provides the best fit to the data. The difference between the log marginal likelihood estimates is equivalent to Bayes factors of the LSTM-SV model compared to the SV and N-SV models of roughly 10^5, strongly supporting the LSTM-SV model. The non-linearity long-memory coefficient β_1 is more than two standard deviations from zero, implying that there is strong evidence of non-linear and long-memory dependence in the volatility dynamics, and that the LSTM structure within the volatility process of the LSTM-SV model is able to capture such dependence.

	μ / β_0	ϕ	σ^2	δ / β_1	Log-mar.llh
SV	0.039(0.317) **2.640**	0.998(0.001) **5.015**	0.069(0.014) **9.910**		−5468.3(0.043)
N-SV	0.059(0.319) **7.097**	0.997(0.001) **10.129**	0.092(0.035) **8.078**	0.017(0.024) **9.048**	−5468.4(0.041)
LSTM-SV	0.552(0.094) **8.883**	0.928(0.01) **7.500**	0.121(0.019) **8.245**	0.131(0.047) **7.266**	−5457.8(0.501)

Table 2: Simulation study: Posterior means of the parameters with the posterior standard deviations in brackets, and the IACT values in bold. The last column shows the estimated log marginal likelihood with the Monte Carlo standard errors in brackets, averaged over 10 different runs of the IS^2 algorithms.

	PPS	# violations	QS	Hit percentage (α=1%)
SV	5.431	22.5	2.028	0.018
N-SV	5.432 (4/10)	22.7 (3/10)	2.029 (6/10)	0.018 (3/10)
LSTM-SV	5.425 (8/10)	19.8 (8/10)	1.995 (8/10)	0.016 (7/10)

Table 3: Experimental study: Forecast performance of the SV, N-SV and LSTM-SV models, averaged over 10 different runs. For the N-SV and LSTM-SV models, the numbers in brackets show the number of times (out of 10 replications) these models have better scores than the SV model.

Table 3 reports the predictive performance scores of the three models, averaged over 10 replications, i.e., 10 different datasets generated from the model in (28) and (29). The LSTM-SV model outperforms the SV and N-SV models for all the predictive scores, which is consistent with the in-sample analysis showing that the LSTM-SV model best fits this simulated dataset. This example illustrates the impressive out-of-sample forecast ability of the LSTM-SV model. The results for the real data applications in the next section further support this claim.

4.2 Applications

This section applies the LSTM-SV model to the three financial time series: the SP500 index, the ASX200 index and the AUD/USD currency exchange rate, which are commonly used as benchmark datasets in the volatility modeling literature to evaluate econometric models.

4.2.1 The datasets and exploratory data analysis

The stock indices SP500, ASX200 and the AUD/USD currency exchange datasets were downloaded from the Yahoo Finance database. We used the adjusted closing prices $\{P_t, t=1,...,T_P\}$

and calculated the demeaned return process as

$$y_t = 100\left(\log\frac{P_{t+1}}{P_t} - \frac{1}{T_P-1}\sum_{i=1}^{T_P-1}\log\frac{P_{i+1}}{P_i}\right), \quad t = 1, 2, ..., T_P - 1, \tag{30}$$

and using the first $T = 1000$ returns for in-sample analysis and the rest for out-of-sample analysis. Table 4 describes the relevant aspects of the datasets.

	Start	End	T_P	Out-of-sample size	Frequency
SP500	4 Jan 1988	23 Nov 2018	1613	612	Weekly
ASX200	22 Nov 1992	18 Nov 2018	1357	356	Weekly
AUD/USD	4 Jan 2010	18 Nov 2018	2231	1230	Daily

Table 4: Descriptions of the SP500, ASX200 and AUD/USD datasets.

	Min	Max	Std	Skew	Kurtosis	$V_n(5)$	$V_n(20)$	$V_n(35)$
SP500	−20.232	11.208	2.229	−0.758	9.685	3.159*	2.353*	1.990*
ASX200	−17.117	9.013	1.978	−0.805	8.453	2.862*	2.099*	1.765*
AUD/USD	−3.884	3.555	0.681	−0.136	4.974	2.406*	1.939*	1.697

Table 5: Descriptive statistics for the demeaned returns of the SP500, ASX200 and AUD/USD datasets. $V_n(q)$, $q = 5$, 20 and 35, shows the test statistics of Lo's modified R/S test of long memory with lag q. The asterisks indicate significance at the 5% level.

Figure 8 in the Appendix plots the time series data and shows the existence of the volatility clustering effect commonly seen in financial data. Table 5 reports some descriptive statistics for these three datasets together with the modified R/S test (Lo, 1991) for long-range memory in the logarithm of the squared returns. Lo's modified R/S test is widely used in the financial time series literature; see, e.g., Lo (1991), Giraitis et al. (2003), Breidt et al. (1998). The SP500 and ASX200 index data exhibit some negative skewness, a high excess kurtosis and a higher variation compared to the exchange rate data. These suggest that there might be non-linear dependence in the volatility dynamics of the index data, while this might not be the case for the exchange rate data. The result of Lo's modified R/S test for long-memory dependence with several different lags q indicates that there is significant evidence of long-memory dependence in the stock indices. For the two stock index datasets, the null hypothesis of short-memory dependence is rejected at the 5% level of significance in all three cases, $q = 5$, 20 and 35. For the exchange rate data, however, the evidence of long memory is less clear as the null hypothesis of short memory is not rejected at the 5% level of significance when $q = 35$. The above exploratory data analysis suggests that there is evidence of non-linear and long-memory dependence in the volatility process of the stock market index data, and that this is not the case for the exchange rate data.

	μ / β_0	ϕ	σ^2	δ / β_1	Log-mar.llh
SP500					
SV	0.716(0.301) **5.996**	0.973(0.015) **9.854**	0.043(0.015) **4.177**		−2061.7(0.025)
N-SV	0.675(0.308) **7.016**	0.971(0.016) **12.068**	0.044(0.015) **2.966**	0.064(0.141) **4.644**	−2061.5(0.026)
LSTM-SV	0.089(0.018) **4.664**	0.931(0.010) **4.576**	0.077(0.012) **4.514**	0.184(0.024) **4.500**	−2060.7(0.520)
ASX200					
SV	0.687(0.295) **5.635**	0.975(0.013) **10.103**	0.036(0.012) **5.628**		−2045.4(0.049)
N-SV	0.772(0.246) **6.266**	0.965(0.017) **11.647**	0.037(0.012) **1.853**	−0.062(0.127) **13.612**	−2045.6(0.053)
LSTM-SV	0.093(0.018) **4.567**	0.926(0.011) **4.580**	0.075(0.011) **4.599**	0.182(0.024) **4.490**	−2045.1(0.311)
AUD/USD					
SV	−0.509(0.196) **5.946**	0.966(0.013) **7.110**	0.035(0.008) **3.941**		−1110.7(0.020)
N-SV	−0.546(0.212) **6.765**	0.961(0.012) **8.036**	0.037(0.013) **4.355**	−0.203(0.126) **3.595**	−1109.9(0.029)
LSTM-SV	−0.060(0.013) **3.724**	0.921(0.010) **3.755**	0.081(0.017) **3.619**	0.143(0.058) **3.465**	−1113.4(0.389)

Table 6: Applications: Posterior means of the parameters with the posterior standard deviations in brackets, and their IACT values in bold. The last column shows the estimated log marginal likelihood with the estimated standard errors in brackets.

4.2.2 In-sample analysis

Table 6 summarizes the estimation results of fitting the SV, N-SV and LSTM-SV models to the three datasets. For the LSTM-SV model, we only show the results of the key parameters and put the rest in Table 10 of the Appendix. We draw some conclusions from Table 6. First, the relatively small IACT values of all the parameters across the three datasets show that the Markov chains mix well and that the BPM sampler is efficient for the SV, N-SV and LSTM-SV models. Second, the marginal likelihood estimates show that the LSTM-SV model fits the index data best, but this is not the case for the exchange rate data. This is consistent with the conclusions of the exploratory data analysis in Section 4.2.1, where the volatility process of the exchange rate data suggests that there is no non-linear and long-memory dependence for the LSTM mechanism to capture. Third, the estimation result for the non-linearity long-memory parameter β_1 of the LSTM-SV model provides further evidence of the non-linearity long-memory effect in the index data. The estimated value of β_1 is far beyond three standard deviations from zero for the index SP500 and ASX200 datasets, but less than three standard deviations from zero for the exchange rate data. Finally, it is worth noting that, in all cases,

the persistence parameter ϕ in the LSTM-SV model is smaller than the persistence parameters in the SV and N-SV models, as the long-term memory is stored in the η_t process by the LSTM architecture.

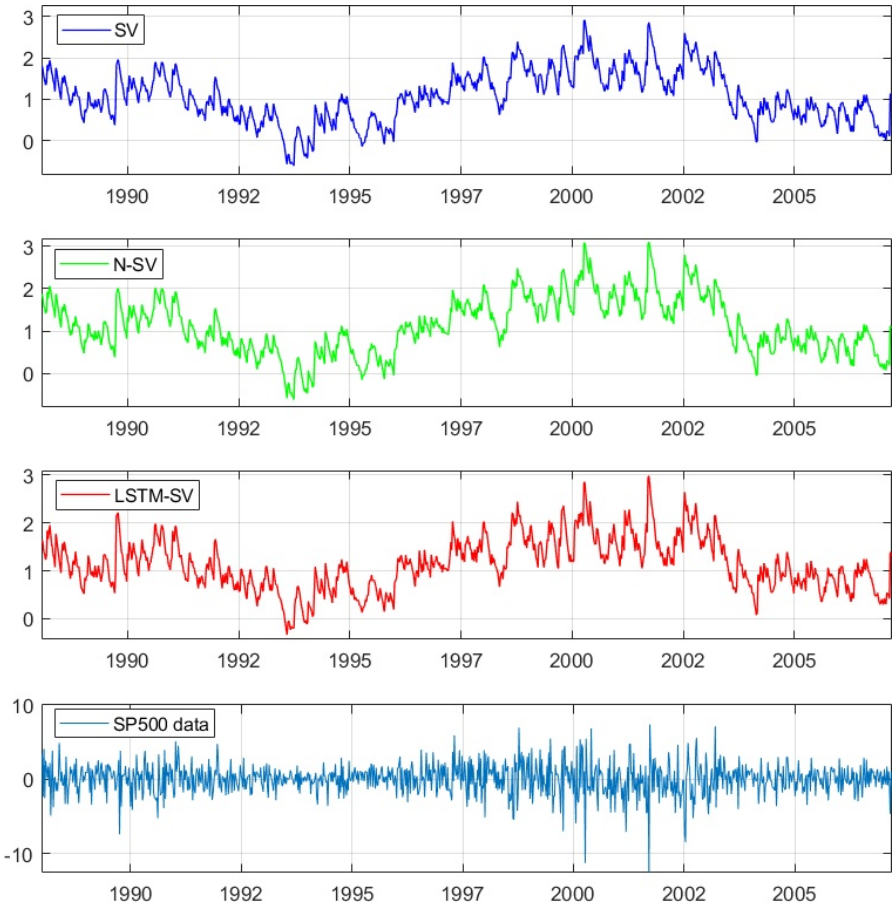

Figure 3: SP500: Plots of the filtered volatility processes and the data.

Using the posterior mean estimates in Table 6, the *filtered* volatilities of the three models can be estimated using the particle filter. Table 7 summarizes the means and standard deviations of the filtered volatilities, with the filtered volatilities of the LSTM-SV model always having the smallest standard deviations in all three datasets. Figures 3, 9 and 12 in the Appendix show the filtered volatility processes together with the in-sample data for the SP500, AXS200 and AUD/USD returns, respectively. In general, the three filtered volatility processes produced by the three models have a similar pattern and adequately capture the volatility clustering effect. However, a closer look at these figures reveals that the SV and N-SV models produce a smaller volatility in low volatility regions, and in general a higher volatility in high volatility regions; see also Figures 5, 11 and 14 where the *forecast* volatilities of the LSTM-SV model are not too small in low volatility regions while not too high in high volatility regions. This suggests that the LSTM-SV model is able to maintain a long-range memory, and is less sensitive to data in shorter periods.

Figures 4, 10 and 13 in the Appendix plot the estimated residuals $\widehat{\epsilon}_t^y$ and their QQ-plots, and Table 8 provides their skewness and kurtosis statistics together with the p-values of the Ljung-Box (LB) autocorrelation test. The results are mixed. The QQ-plots show that the

	SP500		ASX200		AUD/USD	
	Mean	std	Mean	std	Mean	std
SV	1.081	0.633	1.046	0.610	−0.664	0.532
N-SV	1.127	0.668	1.004	0.546	−0.762	0.605
LSTM-SV	1.146	0.540	1.142	0.520	−0.767	0.504

Table 7: Applications: Means and standard deviations of filtered volatilities estimated from the SV, N-SV and LSTM-SV models.

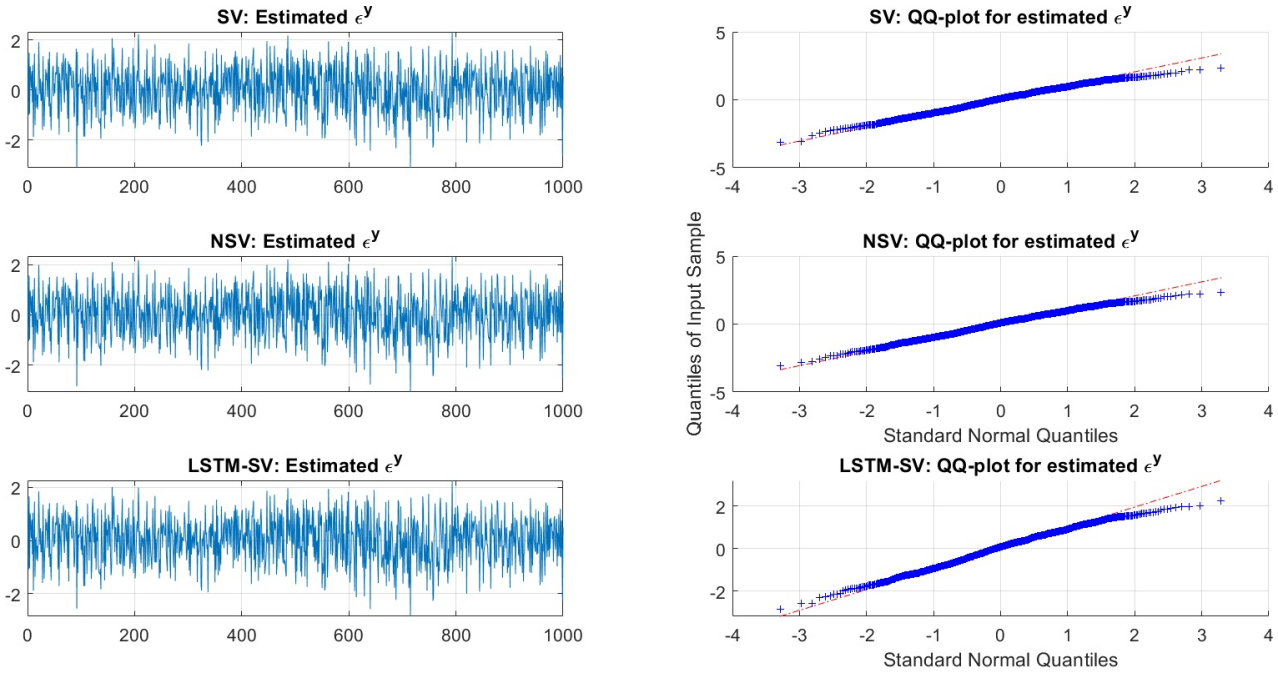

Figure 4: SP500: Residuals and their QQ plots

three models perform quite well, but there are still some outliers that cannot be explained by the models. Similarly to Kim et al. (1998) and Yu et al. (2006), we find that these outliers correspond to the extremely small and large values of $|y_t|$. A small p-value in the LB test shows evidence of autocorrelation between the residuals. Hence, the p-values in Table 8 indicate some evidence of autocorrelation between the residuals for the SP500 data, but not for the other two datasets. That is, there is still some autocorrelation structure in the SP500 indices that is not being detected by any of the SV, N-SV and LSTM-SV methodologies. All the kurtosis values are close to each other, and close to 3, the kurtosis of the standard normal distribution. The residuals exhibit some negative skewness in all cases. We conjecture that extending the LSTM-SV model by using a Student-t distribution instead of a Gaussian for the measurement shock ϵ_t^y and taking into account the leverage effect by correlating ϵ_t^y with the volatility shock ϵ_t^η, is likely to lead to better diagnostic outcomes for the residuals. However, we do not consider these extensions here.

	Skew	Kurtosis	LB p-value
SP500			
SV	−0.169(0.005)	2.528(0.019)	0.052(0.003)
N-SV	−0.290(0.009)	2.615(0.019)	0.052(0.002)
LSTM-SV	−0.290(0.010)	2.519(0.023)	0.046(0.003)
ASX200			
SV	−0.298(0.008)	2.676(0.032)	0.977(0.002)
N-SV	−0.295(0.010)	2.626(0.032)	0.980(0.002)
LSTM-SV	−0.292(0.010)	2.628(0.047)	0.985(0.001)
AUD/USD			
SV	−0.104(0.002)	2.622(0.010)	0.956(0.003)
N-SV	−0.106(0.005)	2.618(0.012)	0.955(0.004)
LSTM-SV	−0.099(0.004)	2.484(0.009)	0.956(0.002)

Table 8: Applications: Model diagnostics of the errors $\widehat{\epsilon}_t^y$. The LB p-values denote the p-value from the Ljung-Box test with 10 lags. The numbers in brackets are MC standard errors across 10 different runs.

Out-of-sample analysis

Figure 5 plots the 99% one-step-ahead forecast intervals on the out-of-sample data of the SP500 returns. See Figures 11 and 14 in the Appendix for the ASX200 and exchange rate data. Overall, the three models have similar forecast bands. However, we note that both the SV and N-SV models, compared to the LSTM-SV model, produce a smaller forecast volatility in low volatility regions and a higher volatility forecast in high volatility regions. This is similar to the filtered volatility discussed before. The figure also shows that the SV and N-SV forecasts depend mainly on the return at the previous step, as the persistence parameters ϕ in the SV and N-SV models are larger than the persistence parameter of the LSTM-SV model. The LSTM-SV intervals seem to track the returns better, especially during the high volatility periods. Readers are encouraged to examine the zoomed-in plot in Figure 6 to convince themselves. The LSTM-SV model gives a safe buffer against abrupt changes in low volatility regions, because it maintains a wider forecast band, while it does not produce overly large forecast intervals in high volatility regions. Therefore, the LSTM-SV model is less sensitive to the data values in the shorter time periods, and maintains a good trade-off between the information in recent observations and the information in the long-term memory.

Table 9 shows the out-of-sample performance of the LSTM-SV, SV and N-SV models. The table suggests that the LSTM-SV model consistently has the best out-of-sample performance in all the predictive measures for the index SP500 and ASX200 data. For the exchange rate data, the LSTM-SV model has a similar performance to the SV model, with the N-SV model slightly better than the other two. This is consistent with the in-sample performance discussed earlier. Our analysis indicates that the underlying volatility dynamics in the exchange rate data is different than that of the index data. It is likely that the latent volatility process of the AUD/USD exchange rate data does not exhibit non-linear and long-memory dependence

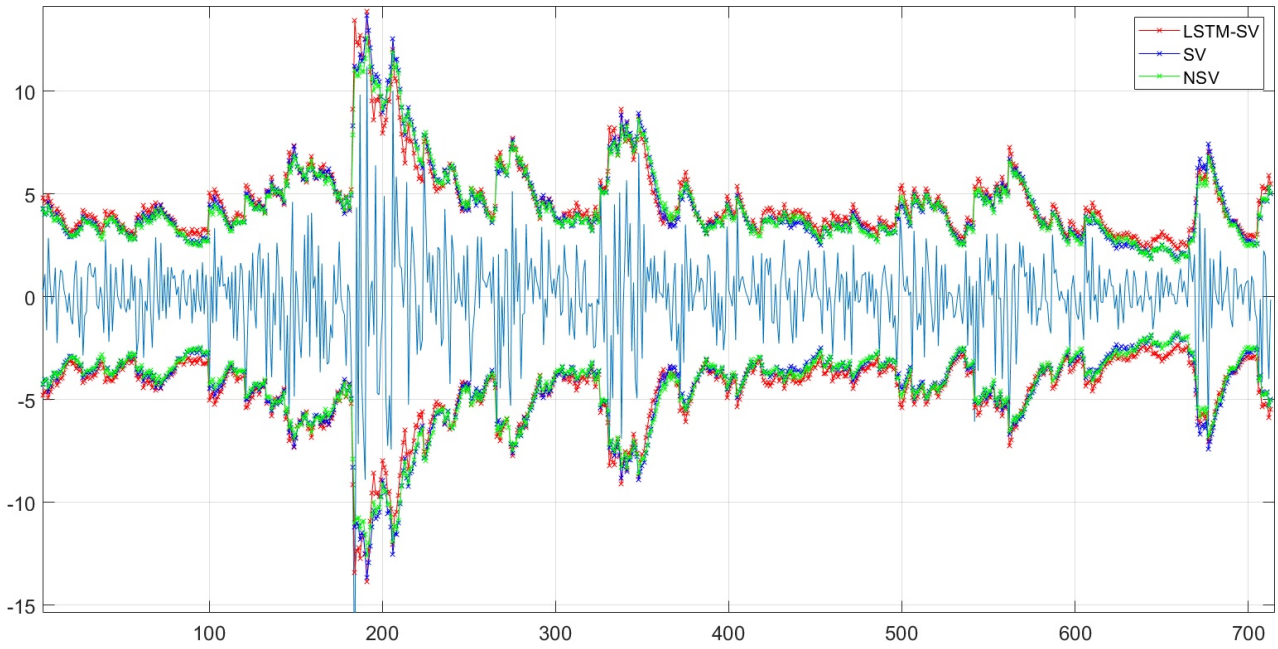

Figure 5: SP500: 99% one-step-ahead forecast intervals on the test data. (This is better viewed in colour).

similar to that observed in the volatility dynamics of the SP500 and ASX200 returns.

5 Conclusions

This paper proposes a long short-term memory stochastic volatility (LSTM-SV) model, by combining the LSTM and SV models in a principled way. We use the Blocking Pseudo Marginal method to sample from the posterior distribution of the LSTM-SV model and estimate the marginal likelihood, for model choice, using the Importance Sampling Squared algorithm. The simulation and empirical studies suggest that the LSTM-SV model is able to capture the potential long-memory and non-linear dependence in volatility dynamics, and is able to produce highly accurate forecast volatilities. Our analysis also reveals a significant difference in the dynamics of the underlying volatility processes between the stock index SP500, ASX200 datasets and the AUD/USD exchange rate data.

Extending the LSTM-SV model by incorporating features such as the leverage effect is an interesting research question. Another interesting research question is extending the present LSTM-SV model to multivariate financial time series. We conjecture that the LSTM architecture will be more powerful for multivariate inputs as it can naturally capture the interaction between the inputs. This research is in progress.

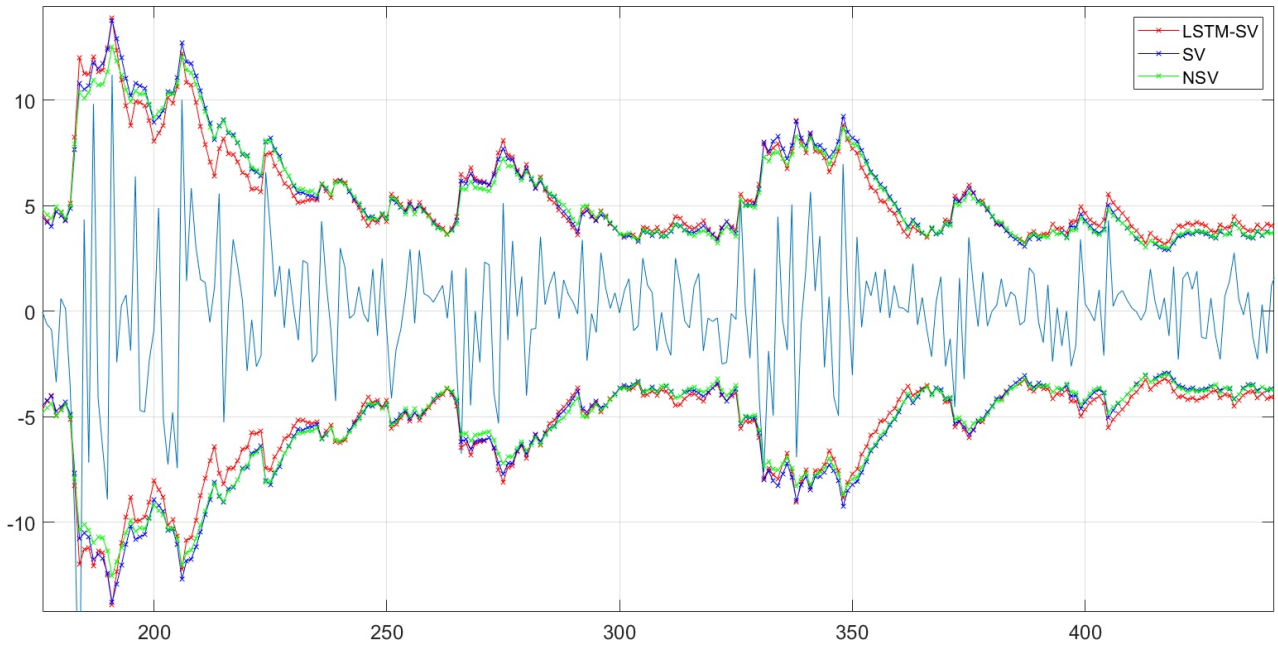

Figure 6: SP500: A zoomed-in of the 99% one-step-ahead forecast intervals on the test data. (This is better viewed in colour).

	PPS	# violations	QS	Hit percentage (α=1%)
SP500				
SV	2.170	17	0.107	0.033
N-SV	2.166	16	0.106	0.033
LSTM-SV	2.154	11	0.092	0.021
ASX200				
SV	1.926	7	0.064	0.022
N-SV	1.925	5	0.064	0.022
LSTM-SV	1.922	4	0.060	0.014
AUD/USD				
SV	0.883	17	0.017	0.009
N-SV	0.880	16	0.017	0.009
LSTM-SV	0.887	16	0.018	0.009

Table 9: Applications: Forecast performance of the SV, N-SV and LSTM-SV models.

Appendix

The LSTM-SV model

The LSTM-SV model in Section 2.3 is fully written as

$$
\begin{aligned}
y_t &= e^{\frac{1}{2}z_t}\epsilon_t^y, \;\; \epsilon_t^y \overset{iid}{\sim} \mathcal{N}(0,1), \;\; t = 1,2,...,T \\
z_t &= \eta_t + \phi z_{t-1}, \;\; t = 2,...,T, \;\; z_1 = \eta_1 \\
\eta_t &= \beta_0 + \beta_1 h_t + \epsilon_t^\eta, \;\; \epsilon_t^\eta \overset{iid}{\sim} \mathcal{N}(0,\sigma^2), \;\; t = 1,2,...,T \\
h_t &= g_t^o \odot tanh(C_t) \\
C_t &= g_t^f \odot C_{t-1} + g_t^i \odot x_t^d \\
g_t^f &= \sigma(v_f \eta_{t-1} + w_f h_{t-1} + b_f) \\
g_t^i &= \sigma(v_i \eta_{t-1} + w_i h_{t-1} + b_i) \\
x_t^d &= \sigma(v_d \eta_{t-1} + w_d h_{t-1} + b_d) \\
g_t^o &= \sigma(v_o \eta_{t-1} + w_o h_{t-1} + b_o),
\end{aligned}
$$

where $\sigma(\cdot)$ is the sigmoid function and $\odot$ denotes element-wise multiplication. The model parameter vector is $\theta = (\beta_0,\beta_1,\phi,\sigma^2,v_f,w_f,b_f,v_i,w_i,b_i,v_d,w_d,b_d,v_o,w_o,b_o)$. The log density of y_t given θ and z_t is

$$
\log p_\theta(y_t|z_t) = -\frac{1}{2}\log 2\pi - \frac{1}{2}z_t - \frac{y_t^2}{2e^{z_t}}. \tag{31}
$$

Figure 7 plots the graphical representation of the LSTM-SV model.

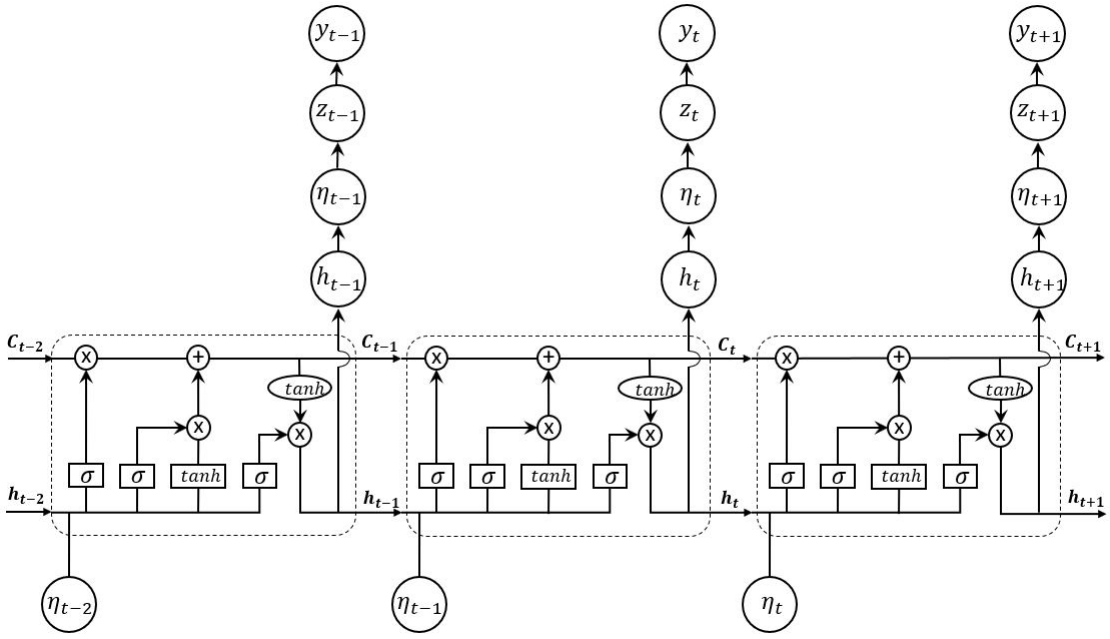

Figure 7: Graphical representation of the LSTM-SV model.

The particle filter for the LSTM-SV model

Algorithm 3 describes the particle filter for the LSTM-SV model using $\mathbf{Z}_t=(Z_t^1,...,Z_t^N)$ to denote the vector of particles at time t. The set of standard normal random numbers U includes two sources of randomness: the set of random numbers $\{U_{t,k}^P,t=1,...,T;k=1,...,N\}$ used to propose new particles in each time step, and the set of random numbers $\{U_{t,k}^R,t=1,...,T-1;k=1,...,N\}$ used in the resampling step. For the resampling step, we use multinomial resampling, with sorting, to obtain the vector ancestor indexes $\{A_{t-1}^k,k=1,...,N\}$ used to propose particles at time t. The sorting step helps eliminate the discontinuity issues of the selected particles in the ordinary multinomial resampling scheme (Gerber and Chopin, 2014). This sorted resampling scheme allows the selected particles to still be close after being resampled and hence helps to reduce the variability of the likelihood ratio estimator $\widehat{p}(y_{1:T}|\theta',u')/\widehat{p}(y_{1:T}|\theta,u)$ shown in the Algorithm 1 (Deligiannidis et al., 2018).

The multinomial resampling scheme in step 2a and 2b generates the ancestor index $A_{t-1}^k,k=1,...,N$, from the multinomial distribution denoted as $\mathcal{F}(\cdot|\mathbf{p},\mathbf{u})$ with $\mathbf{p}$ the vector of parameters of the multinomial distribution and $\mathbf{u}$ the uniform random numbers used within a multinomial random number generator. We use the standard normal cumulative distribution function $\Phi(\cdot)$ in the resampling step to transform the normal random numbers $U_{t-1,k}^R$ to the uniform random numbers, denoted as $\overline{U}_{t-1,k}^R$.

Algorithm 3 Particle filter for the LSTM-SV model

Input: $T,N,y_{1:T},\theta,U=(U^P_{1,1},...,U^P_{T,N},U^R_{1,1},...,U^R_{T-1,N})$

1. At time $t=1$,

   (a) for $k=1,...N$, initialize the particles (H^k_1,η^k_1,Z^k_1), e.g., $H^k_1=0$, as the LSTM cell initially has no memory, and

   $$\begin{aligned} \eta^k_1 &= \beta_0+\sigma U^P_{1,k} \\ Z^k_1 &= \eta^k_1 \end{aligned}$$

   (b) compute and normalize the weights

   $$\begin{aligned} w_1(Z^k_1) &= \frac{\mu_\theta(Z^k_1)g_\theta(y_1|Z^k_1)}{q_\theta(Z^k_1|y_1)}=g_\theta(y_1|Z^k_1) \\ W^k_1 &= \frac{w_1(Z^k_1)}{\sum_{m=1}^N w_1(Z^m_1)} \end{aligned}$$

   (c) compute the estimated likelihood $\widehat{p}(y_1|\theta)$ as

   $$\widehat{p}(y_1|\theta,U)=\frac{1}{N}\sum_{k=1}^N w_1(Z^k_1).$$

2. At times $t=2,...,T$,

   (a) sort the particle vector $\mathbf{Z}_{t-1}$ in ascending order to obtain the vector of sorted particles $\overline{\mathbf{Z}}_{t-1}=(\overline{Z}^1_{t-1},...,\overline{Z}^N_{t-1})$. The sorted index vector associated with $\overline{\mathbf{Z}}_{t-1}$ is denoted as $\mathbf{I}_{t-1}=(I^1_{t-1},...,I^N_{t-1})$. In this setting, we have the relation $\overline{Z}^k_{t-1}=Z^{I^k_{t-1}}_{t-1}$ with $k=1,...,N$. Use the sorted index vector $\mathbf{I}_{t-1}$ to define the vector of sorted weights $(\overline{W}^1_{t-1},...,\overline{W}^N_{t-1})$ such that

   $$\overline{W}^k_{t-1} = W^{I^k_{t-1}}_{t-1}$$

   (b) sample $A^k_{t-1}\sim\mathcal{F}(\cdot|\overline{W}^k_{t-1},\overline{U}^R_{t-1,k})$ where $\overline{U}^R_{t-1,k}=\Phi(U^R_{t-1,k})$ for $k=1,...,N$.

(c) for $k=1,...N$, generate particles Z_t^k by

$$\begin{aligned} H_t^k &= \text{LSTM}(\eta_{t-1}^{A_{t-1}^k}, H_{t-1}^{A_{t-1}^k}) \\ \eta_t^k &= \beta_0 + \beta_1 H_t^k + \sigma U_{t,k}^P \\ Z_t^k &= \eta_t^k + \phi Z_{t-1}^{A_{t-1}^k} \end{aligned}$$

and set $Z_{1:t}^k = (Z_{1:t-1}^{A_{t-1}^k}, Z_t^k)$.

(d) compute and normalize the weights

$$\begin{aligned} w_t(Z_{1:t}^k) &= \frac{f_\theta(Z_t^k | Z_{t-1}^{A_{t-1}^k}) g_\theta(y_t | Z_t^k)}{q_\theta(Z_t^k | y_t, Z_{t-1}^{A_{t-1}^k})} = g_\theta(y_1 | Z_1^k) \\ W_t^k &= \frac{w_t(Z_{1:t}^k)}{\sum_{m=1}^N w_t(Z_{1:t}^m)} \end{aligned}$$

(e) compute the estimated likelihood $\widehat{p}(y_t | y_{1:t-1}, \theta)$ as

$$\widehat{p}(y_t | y_{1:t-1}, \theta, U) = \frac{1}{N} \sum_{k=1}^N w_t(Z_{1:t}^k).$$

Output: Estimate of the likelihood

$$\widehat{p}(y_{1:T} | \theta, U) = \widehat{p}(y_1 | \theta, U) \prod_{t=2}^T \widehat{p}(y_t | y_{1:t-1}, \theta, U).$$

Additional results for section 4.2

Table 10 summarizes the estimation results for all the LSTM parameters in all the examples.

	Simulation	SP500	ASX200	AUD/USD
v_d	-0.421(0.244)	0.412(0.199)	0.037(0.230)	0.412(0.200)
w_d	-0.072(0.286)	-0.357(0.168)	-0.245(0.217)	-0.357(0.168)
b_d	0.401(0.222)	-0.043(0.188)	-0.138(0.110)	-0.043(0.188)
v_i	-0.266(0.189)	-0.086(0.194)	-0.198(0.218)	-0.086(0.194)
w_i	-0.074(0.242)	0.342(0.180)	0.350(0.105)	0.342(0.180)
b_i	-0.413(0.219)	-0.125(0.196)	-0.082(0.204)	-0.125(0.196)
v_o	0.142(0.285)	-0.235(0.210)	-0.146(0.197)	-0.235(0.210)
w_o	0.162(0.272)	0.003(0.209)	-0.290(0.212)	0.002(0.209)
b_o	0.178(0.276)	-0.468(0.049)	-0.435(0.183)	-0.468(0.049)
v_f	0.228(0.272)	0.632(0.066)	0.267(0.212)	0.632(0.066)
w_f	0.159(0.247)	0.065(0.169)	-0.023(0.260)	0.065(0.169)
b_f	0.270(0.276)	-0.291(0.074)	-0.420(0.210)	-0.291(0.074)
$\text{IACT}_{\max}$	9.619	4.641	4.942	3.798
$\text{IACT}_{\min}$	7.056	4.200	4.354	3.460

Table 10: Posterior means and max and min IACT values for the LSTM parameters of the LSTM-SV model. The numbers in the brackets are posterior standard deviations.

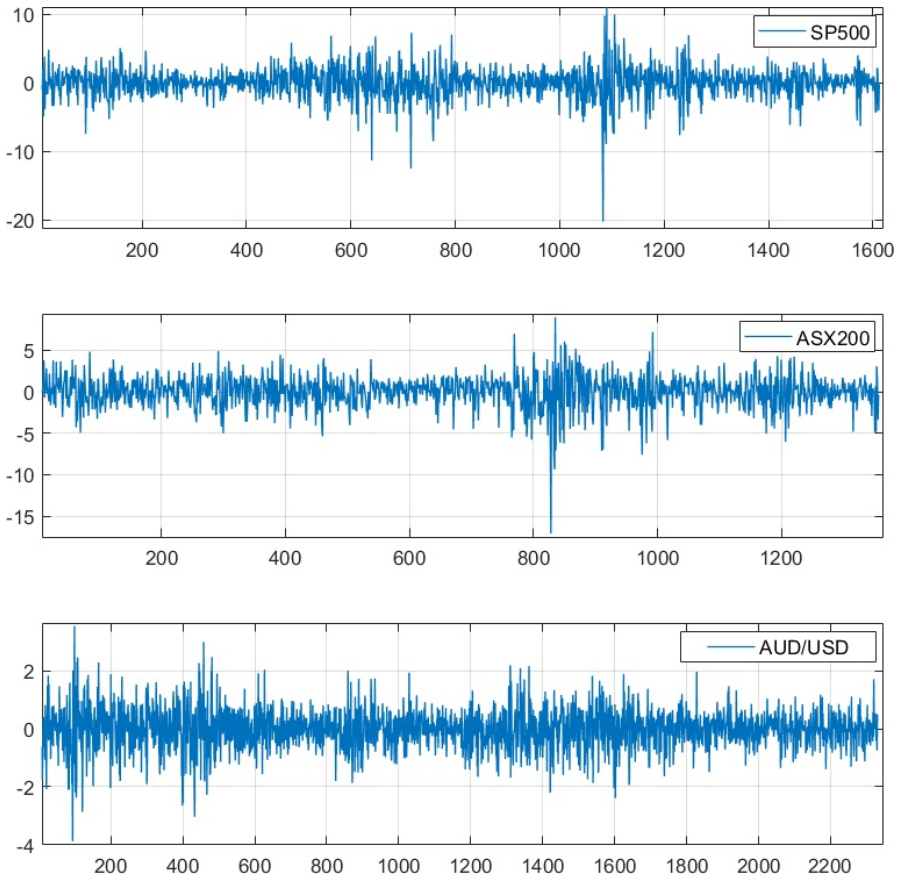

Figure 8: Applications: Time series plots for the SP500, ASX200 and AUS/USD exchange rate datasets.

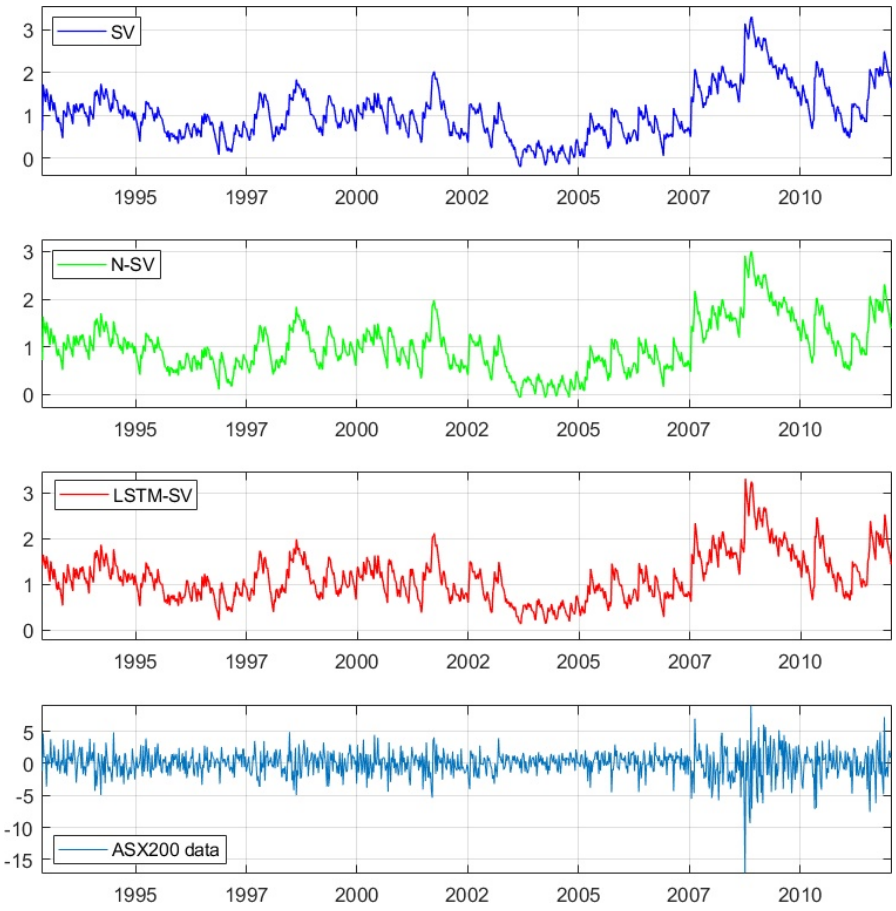

Figure 9: ASX200: Filtered volatility processes and the data.

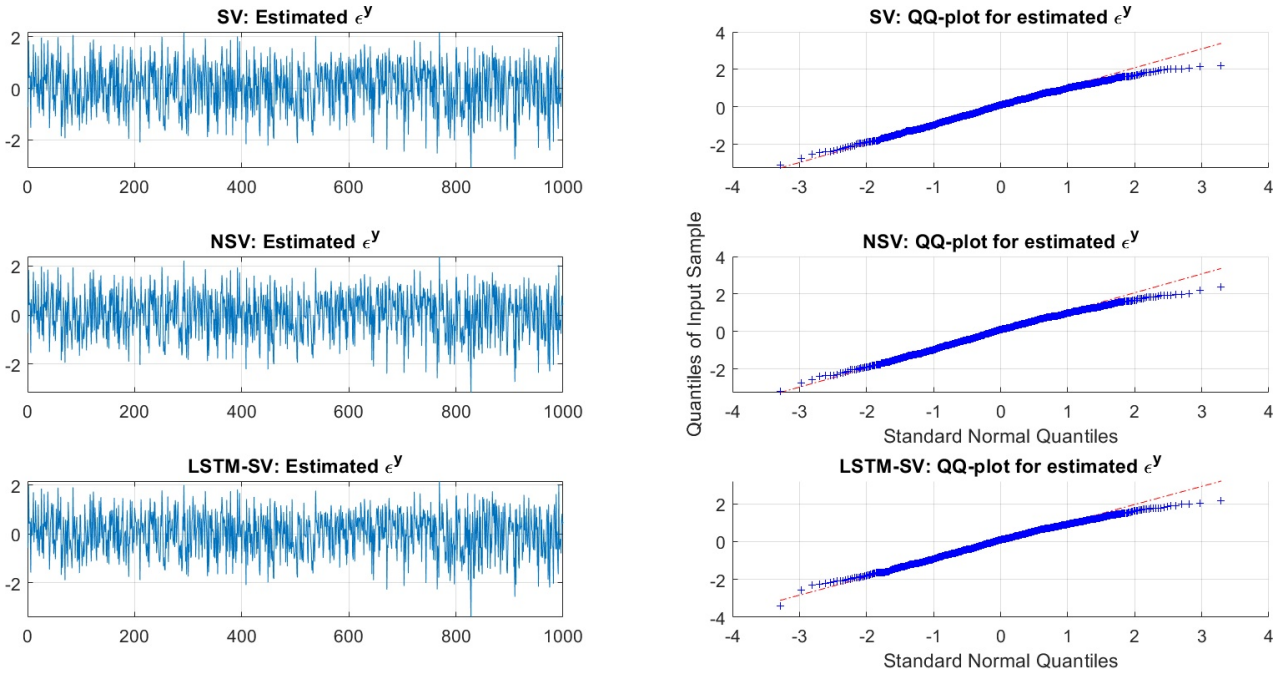

Figure 10: ASX200: Residual and QQ plots

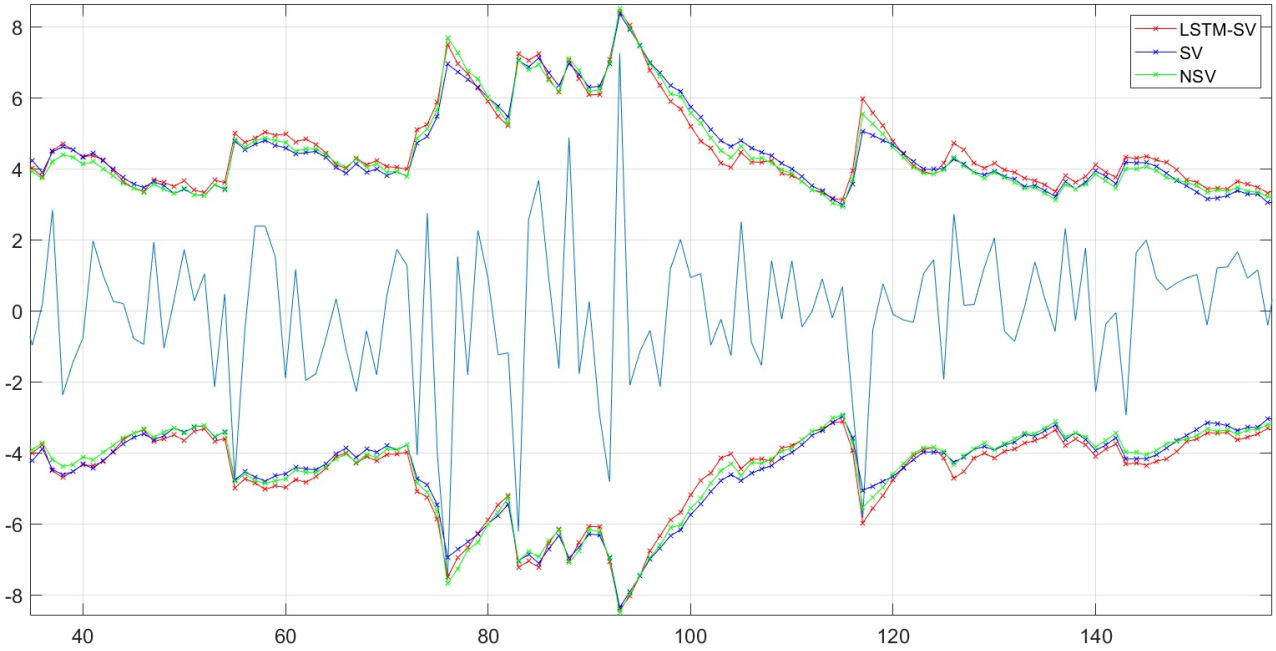

Figure 11: ASX200: A zoomed-in of the 99% one-step-ahead forecast intervals on the test data. (This is better viewed in colour).

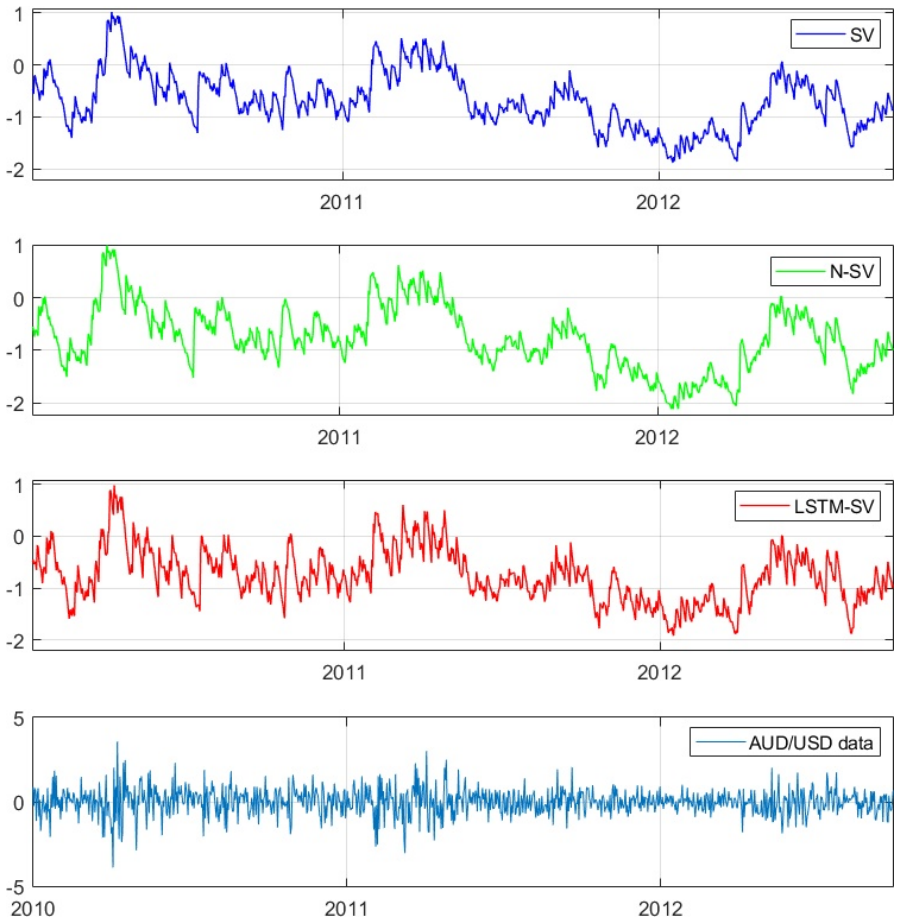

Figure 12: AUD/USD Exchange rate: Filtered volatility processes and the data.

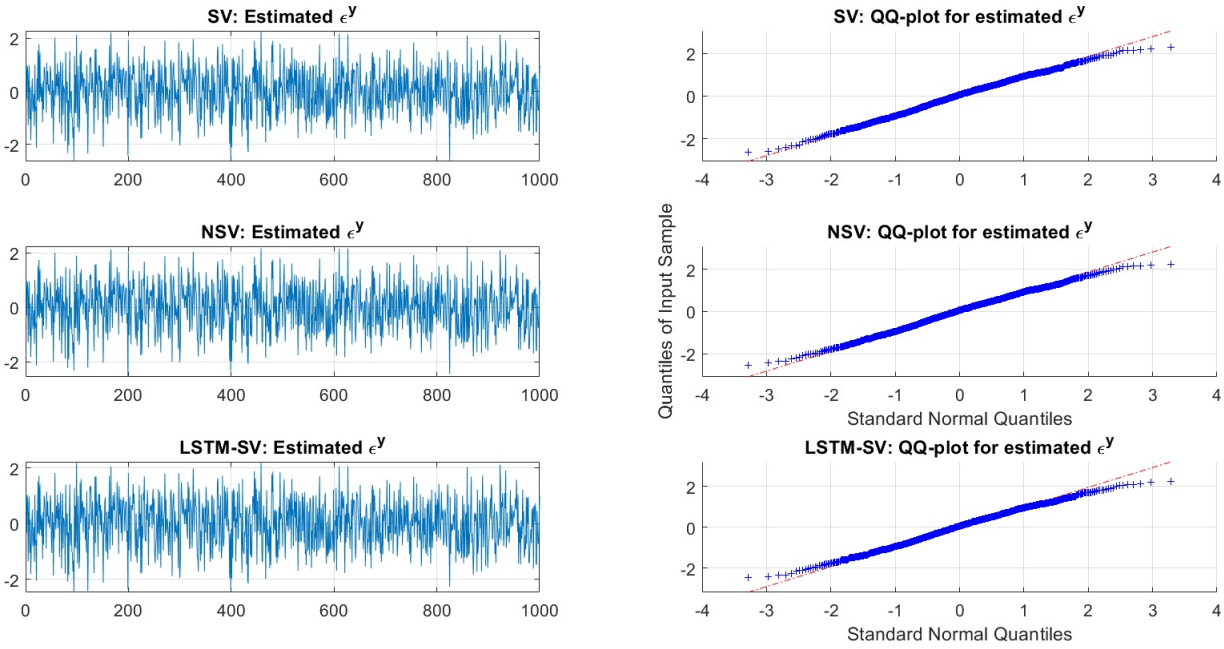

Figure 13: AUD/USD Exchange rate: Residual and QQ plots

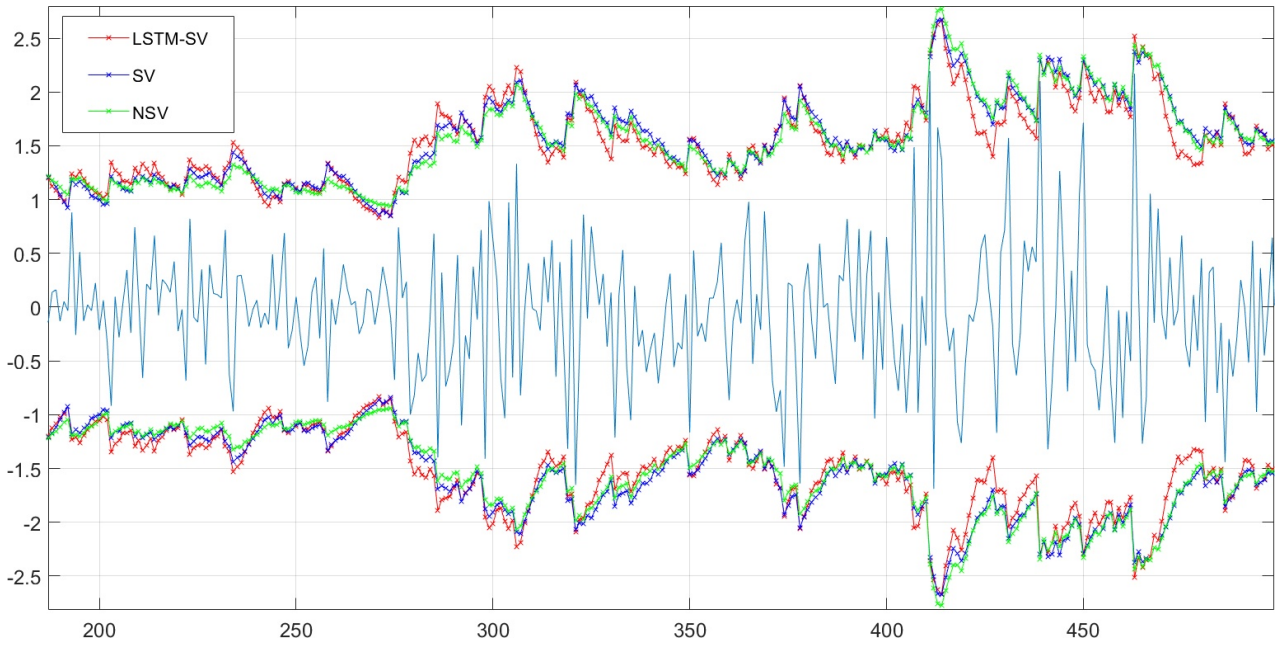

Figure 14: AUD/USD Exchange rate: A zoomed-in of the 99% one-step-ahead forecast intervals on the test data. (This is better viewed in colour).

References

Andrieu, C., Doucet, A., and Holenstein, R. (2010). Particle Markov chain Monte Carlo methods. *Journal of the Royal Statistical Society, Series B*, 72:1–33.

Andrieu, C. and Roberts, G. (2009). The pseudo-marginal approach for efficient Monte Carlo computations. *The Annals of Statistics*, 37:697–725.

Bengio, Y., Frasconi, P., and Simard, P. (1993). The problem of learning long-term dependencies in recurrent networks. 3:1183–1188.

Bengio, Y., Simard, P., and Frasconi, P. (1994). Learning long-term dependencies with gradient descent is difficult. *IEEE Transactions on Neural Networks*, 5(2):157–166.

Bollerslev, T. (1986). Generalized autoregressive conditional heteroskedasticity. *Journal of Econometrics*, 31(3):307 – 327.

Bollerslev, T. and Mikkelsen, H. O. (1996). Modeling and pricing long memory in stock market volatility. *Journal of Econometrics*, 73(1):151 – 184.

Breidt, F., Crato, N., and de Lima, P. (1998). The detection and estimation of long memory in stochastic volatility. *Journal of Econometrics*, 83(1):325 – 348.

Crato, N. and de Lima, P. J. (1994). Long-range dependence in the conditional variance of stock returns. *Economics Letters*, 45(3):281 – 285.

Deligiannidis, G., Doucet, A., and Pitt, M. K. (2018). The correlated pseudo marginal method. *Journal of the Royal Statistical Society: Series B (Statistical Methodology)*, 80(5):839–870.

Ding, Z., Granger, C. W., and Engle, R. F. (1993). A long memory property of stock market returns and a new model. *Journal of Empirical Finance*, 1(1):83 – 106.

Elman, J. L. (1990). Finding structure in time. *Cognitive Science*, 14:179–21.

Garthwaite, P., Fan, Y., and Sisson, S. (2010). Adaptive optimal scaling of Metropolis-Hastings algorithms using the Robbins-Monro process. *Communications in Statistics - Theory and Methods*, 45.

Gerber, M. and Chopin, N. (2014). Sequential quasi-monte carlo. *Journal of the Royal Statistical Society: Series B (Statistical Methodology)*, 77.

Gers, F. A., Schmidhuber, J., and Cummins, F. A. (2000). Learning to forget: Continual prediction with LSTM. *Neural Computation*, 12:2451–2471.

Giraitis, L., Kokoszka, P., Leipus, R., and Teyssire, G. (2003). Rescaled variance and related tests for long memory in volatility and levels. *Journal of Econometrics*, 112(2):265 – 294.

Gneiting, T. and Raftery, A. E. (2007). Strictly proper scoring rules, prediction, and estimation. *Journal of the American Statistical Association*, 102(477):359–378.

Good, I. J. (1952). Rational decisions. *Journal of the Royal Statistical Society. Series B (Methodological)*, 14(1):107–114.

Goodfellow, I., Bengio, Y., and Courville, A. (2016). *Deep Learning*. MIT Press.

Granger, C. W. J. and Joyeux, R. (1980). An introduction to long-memory time series models and fractional differencing. *Journal of Time Series Analysis*, 1(1):15–29.

Greff, K., Srivastava, R. K., Koutnk, J., Steunebrink, B. R., and Schmidhuber, J. (2017). LSTM: A search space odyssey. *IEEE Transactions on Neural Networks and Learning Systems*, 28(10):2222–2232.

Hochreiter, S. and Schmidhuber, J. (1997). Long short-term memory. *Neural computation*, 9:1735–80.

Jacquier, E., Polson, N. G., and Rossi, P. E. (1994). Bayesian analysis of stochastic volatility models (with discussion). *Journal of Business and Economic Statistics*, 12:371–417.

Kiliç, R. (2011). Long memory and nonlinearity in conditional variances: A smooth transition FIGARCH model. *Journal of Empirical Finance*, 18(2):368 – 378.

Kim, S., Shephard, N., and Chib, S. (1998). Stochastic volatility: likelihood inference and comparison with ARCH models. *Review of Economic Studies*, 65:361–393.

Lipton, Z., Berkowitz, J., and Elkan, C. (2015). A critical review of recurrent neural networks for sequence learning. arXiv:1804.04359.

Liu, J. S. (2001). *Monte Carlo Strategies in Scientific Computing*. Springer-Verlag New York.

Lo, A. W. (1991). Long-term memory in stock market prices. *Econometrica*, 59(5):1279–1313.

Makridakis, S., Spiliotis, E., and Assimakopoulos, V. (2018). Statistical and machine learning forecasting methods: Concerns and ways forward. *PLOS ONE*, 13(3):1–26.

Mandelbrot, B. (1967). The variation of some other speculative prices. *The Journal of Business*, 40(4):393–413.

Nelson, D. B. (1991). Conditional heteroskedasticity in asset returns: A new approach. *Econometrica*, 59(2):347–370.

Pitt, M. K., dos Santos Silva, R., Giordani, P., and Kohn, R. (2012). On some properties of Markov chain Monte Carlo simulation methods based on the particle filter. *Journal of Econometrics*, 171(2):134 – 151. Bayesian Models, Methods and Applications.

Plummer, M., Best, N., Cowles, K., and Vines, K. (2006). Coda: Convergence diagnosis and output analysis for MCMC. *R News*, 6(1):7–11.

Taylor, J. W. (2019). Forecasting value at risk and expected shortfall using a semiparametric approach based on the asymmetric laplace distribution. *Journal of Business & Economic Statistics*, 37(1):121–133.

Taylor, S. (1986). *Modelling Financial Time Series*. John Wiley, Chichester.

Taylor, S. J. (1982). Financial returns modelled by the product of two stochastic processes a study of daily sugar prices 1961-79. In Anderson, O. D., editor, *Time Series Analysis: Theory and Practice*, page 203226. Amsterdam: North-Holland.

Tran, M.-N., Kohn, R., Quiroz, M., and Villani, M. (2016). Block-wise pseudo-marginal metropolis-hastings. *arXiv:1603.02485*.

Tran, M.-N., Scharth, M., Gunawan, D., Kohn, R., Brown, S. D., and Hawkins, G. E. (2019). Robustly estimating the marginal likelihood for cognitive models via importance sampling. *arXiv:1906.06020*.

van Bellegem, S. (2012). Locally stationary volatility modeling. In Bauwens, L., Hafner, C., and Laurent, S., editors, *Volatility Models and Their Applications*. Wiley & Sons.

Yu, J. (2002). Forecasting volatility in the New Zealand stock market. *Applied Financial Economics*, 12(3):193–202.

Yu, J., Yang, Z., and Zhang, X. (2006). A class of nonlinear stochastic volatility models and its implications for pricing currency options. *Computational Statistics and Data Analysis*, 51(4):2218 – 2231.

Zhang, G. (2003). Time series forecasting using a hybrid ARIMA and neural network model. *Neurocomputing*, 50:159 – 175.